

or down-regulated before IFN therapy were similar to those of healthy volunteers 6 months after the end of IFN therapy (figure 2A, CR group). On the other hand, in the NR group, expression of genes that were either up- or down-regulated before IFN therapy tended to remain up- or down-regulated 6 months after the end of IFN therapy (figure 2A, NR group). This suggests that the changes in gene-expression profiles of patients with CH-C before IFN therapy reflect the state of HCV infection.

We performed real-time PCR to corroborate the microarray data. Real-time PCR revealed that *CD69* was up-regulated in patients with CH-C and that *CCR2* and *IL7R* were down-regulated in patients with CH-C (figure 2B and table 2).

Relationship between PBMC gene-expression profiles and IFN response. We then analyzed the relationship between PBMC gene-expression profiles before the start of IFN therapy and IFN response. Because the regimen of IFN treatment was different in group A and group B patients, we first focused on group A patients (table 1). In hierarchical clustering analysis using all genes before IFN therapy, no clustering was seen in the CR, BR, or NR groups. Conventional supervised learning methods, such as support vector machine and nearest neighbor (BRB-ArrayTools), could not discriminate between the CR, BR, and NR groups. Therefore, we applied the FNN-SWEEP method to predict the outcome of IFN therapy. Before FNN-SWEEP analysis, nonspecific genes or genes with errors were eliminated by the PART method. The 32 genes screened by PART are shown in figure 3. Topoisomerase (DNA) I (*TOPI*) and interleukin 2 receptor β (*IL2RB*) were up-regulated in the CR group, hemoglobin γ G (*HBG2*) and monocyte chemotactic protein were up-regulated in the BR group, and chemokine (C-C motif) ligand 4 and ras-related C3 botulinum toxin substrate 2 (*RAC2*) were up-regulated in the NR group. Genes selected by PART were subjected to the FNN-SWEEP method to construct a class prediction model. Consequently, we selected 10 gene combinations by the SWEEP operator method for CH-C class prediction before the start of IFN therapy (table 4). The most effective gene combination for the prediction of an IFN response was *TOPI*; catenin (cadherin-associated protein) β 1 (88 kD); and *RAC2*. The accuracy of the training and test sets were high, at 91.0% and 89.1%, respectively.

Changes in gene-expression profiles over the course of IFN therapy. We next focused on the changes in gene-expression profiles over the course of IFN therapy and their relationship with IFN response. Using PART, 86 genes with changes in expression between before and 2 weeks after the start of IFN therapy were selected. To investigate the relationship between the 86 genes with changes due to IFN therapy and the efficacy of IFN therapy, changes in the expression of the 86 genes were determined for the CR group. On the basis of self-organizing maps, changes in gene expression in the CR group were clas-

sified into the following 5 patterns (figure 4): pattern A, up-regulated 2 weeks after the start of IFN therapy and then down-regulated after the end of IFN therapy; pattern B, down-regulated 2 weeks after the start of IFN therapy and then up-regulated after the end of IFN therapy; pattern C, up-regulated 2 weeks after the start of IFN therapy and also up-regulated after the end of IFN therapy; pattern D, up-regulated at 2 weeks after the start of IFN therapy and then returned to normal after the end of IFN therapy; and pattern E, down-regulated at 2 weeks after the start of IFN therapy and also down-regulated after the end of IFN therapy. Patterns A and B represent gene groups with temporary changes during IFN therapy, whereas patterns C, D, and E represent gene groups with changes after the end of IFN therapy and are thought to be attributable to viral eradication or normalization of hepatic function. Interestingly, very little change was seen in the patterns for the NR group. Therefore, changes in gene expression are also useful in predicting therapeutic efficacy. From the 86 genes isolated by PART, the SWEEP operator method was used to identify 10 gene combinations, and therapeutic efficacy was predicted according to the FNN-SWEEP method (table 5). The results showed that the accuracy for gene combinations 7, 8, and 9 was high, at 90.2%. LOOCV confirmed the high accuracy (87.9%) of prediction using these gene combinations. These combinations included the following genes that are important for predicting therapeutic efficacy: *CDC20* was classified as belonging to pattern A; cyclin G1 and differentiation 6 were as belonging to pattern B; and *MIHC* and apoptosis inhibitor 1 were as belonging to pattern E (figure 4).

IFN and ribavirin combination therapy. We then investigated the usefulness of the above-mentioned genes in predicting the efficacy of IFN and ribavirin combination therapy. It has been shown that concurrent ribavirin administration improves the rate of CR. In addition, the changes in gene expression during combination therapy are due not only to IFN but also to ribavirin. Thus, the results for monotherapy may not be applicable to combination therapy. However, changes in the expression of several genes—CD2 antigen (p50), *IL2RB*, *HBG2*, myeloid cell nuclear differentiation antigen (*MNDA*), and *STAT1AB*—were shown to be extremely useful for distinguishing CR from NR in IFN and ribavirin combination therapy (tables 3 and 4).

DISCUSSION

HCV load, genotype, and fibrosis have been listed as factors that influence the effectiveness of IFN therapy [4, 5], but these factors are not sufficient, and other predictive factors are needed. Unlike liver-biopsy specimens, PBMCs can be easily collected, and collection can be repeated as necessary. We analyzed the gene-expression profiles of PBMCs in patients with CH-C by use of cDNA microarrays under the hypothesis that

gene expression in PBMCs is indicative of IFN efficacy and CH-C disease state. In addition, changes in the gene-expression profiles of PBMCs were analyzed during the course of IFN therapy to clarify the relationship between gene-expression profiles of PBMCs and IFN response.

Interestingly, the gene-expression profiles of PBMCs from patients with CH-C and from healthy volunteers were different, and this was confirmed by hierarchical clustering analysis and supervised learning analysis using support vector machine. When patients with CH-C and healthy volunteers were compared, gene expression in the JAK-STAT cascade, humoral immune response, and G protein-coupled receptor protein signaling pathway differed markedly. In most patients with CH-C, expression of these genes is activated, and HCV infection is thought to bring about changes in the gene expression in PBMCs. Several chemokine- and cytokine-related genes, such as *CCR2* and *IL7R*, were down-regulated. Although the reason for this was not clear, expression of these genes in liver-infiltrating lymphocytes was up-regulated. Therefore, the down-regulation of immune-related genes may represent increased levels of liver-infiltrating lymphocytes accompanying hepatitis. Interestingly, when the chronological changes in PBMC gene-expression profiles were analyzed for the CR group, the profiles at 6 months after the end of therapy were similar to those of healthy volunteers. Therefore, the changes in gene-expression profiles before IFN therapy were due to HCV infection. On the other hand, the gene-expression profiles of the NR group before IFN therapy were similar to those at 6 months after the end of IFN therapy (figure 2A).

Unfortunately, it was not possible to differentiate between CR, BR, and NR patients on the basis of gene-expression profiles of PBMCs by use of nonsupervised learning methods, such as hierarchical clustering, before IFN therapy. Therefore, we used FNN theory for CH-C class prediction. The most attractive feature of FNN is that causality between input and output variables can be described very accurately as explicit if-then rules obtained from the constructed model. For the purpose of analyzing numerous genes in a short time, FNN combined with the SWEEP operator method was developed (FNN-SWEEP method) and has been shown to be a precise, simple tool for predicting patient survival on the basis of microarray data [28, 29]. In addition, by first filtering genes by use of PART, the accuracy of the FNN-SWEEP method was further increased [30]. In the present study, a total of 32 genes were identified by PART on the basis of genetic changes before therapy, and, in the CR group, expression of genes such as *TOP1*, *IL2RB*, prothymosin α (*PTMA*), and ADP-ribosyltransferase was up-regulated, thus indicating active cellular proliferation. In the NR group, the expression of genes indicating activated cytotoxic T cells—such as granzyme, CD2 antigen, *RAC2*, and natural killer cell transcript 4—was up-regulated. Because these

genes were up-regulated by IFN therapy in the CR group, they were thought to be up-regulated before therapy in the NR group. Lempicki et al. reported elevated expression of endogenous IFN/innate immune response genes in PBMCs from NR patients coinfecting with HCV and HIV [31]. This suggests that, in many NR patients, few immune effector cells are active or that these effector cells cannot infiltrate the liver and remain in the peripheral blood.

To further investigate the above-mentioned points, changes in the gene-expression profiles of PBMCs were determined during the course of IFN therapy. On the basis of expression profiles before and 2 weeks after the start of IFN therapy, 86 genes were selected. These genes did not include as many IFN- α -stimulated genes as were noted in liver [25–27] (table 6), but they included valuable immune regulatory genes.

On the basis of self-organizing maps, changes in gene expression in the CR group were then classified into 5 patterns (figure 4). These gene groups represent genes with temporary changes due to IFN therapy and those with changes after the end of IFN therapy. Gene groups with changes after the end of IFN therapy are thought to be involved in viral eradication or the normalization of hepatic function. Interestingly, little change was seen in any of the patterns in the NR group. In efficacy prediction by the FNN-SWEEP method, the accuracy for the gene combinations 7, 8, and 9 was high, at 90.2%, thus suggesting that changes in gene expression 2 weeks after the start of IFN therapy are also useful in predicting therapeutic efficacy.

We also investigated whether these genes are useful in predicting the efficacy of IFN and ribavirin combination therapy. Changes in gene expression during combination therapy were due not only to IFN but also to ribavirin, and the results for monotherapy could not simply be applied to combination therapy. However, changes in the expression of several genes—CD2 antigen (p50), *IL2RB*, *HBG2*, *MNDA*, and *STAT1AB*—were shown to be extremely useful for distinguishing CR from NR in IFN and ribavirin combination therapy.

Unfortunately, because the number of subjects in the present study was small, the genes that were identified as predictors for IFN monotherapy were not necessarily predictors for IFN and ribavirin combination therapy. However, the present study was the first to show that responses to IFN therapy could be predicted on the basis of changes in gene expression by PBMCs, and further investigations in greater numbers of patients are required.

Acknowledgments

We thank Prof. Kenichi Kobayashi, for helpful discussion and advice. We also thank A. Nakano, M. Ueda, and J. Hara, for their valuable technical assistance.

References

1. McHutchison JG, Gordon SC, Schiff ER, et al. Interferon alfa-2b alone or in combination with ribavirin as initial treatment for chronic hepatitis C. Hepatitis Interventional Therapy Group. *N Engl J Med* 1998; 339:1485–92.
2. Davis GL, Esteban-Mur R, Rustgi V, et al. Interferon alfa-2b alone or in combination with ribavirin for the treatment of relapse of chronic hepatitis C. International Hepatitis Interventional Therapy Group. *N Engl J Med* 1998; 339:1493–99.
3. Poynard T, Marcellin P, Lee SS, et al. Randomised trial of interferon alpha2b plus ribavirin for 48 weeks or for 24 weeks versus interferon alpha2b plus placebo for 48 weeks for treatment of chronic infection with hepatitis C virus. International Hepatitis Interventional Therapy Group. *Lancet* 1998; 352:1426–32.
4. Martinot-Peignoux M, Marcellin P, Pouteau M, et al. Pretreatment serum hepatitis C virus RNA levels and hepatitis C virus genotype are the main and independent prognostic factors of sustained response to interferon alfa therapy in chronic hepatitis C. *Hepatology* 1995; 22: 1050–6.
5. Tsubota A, Chayama K, Ikeda K, et al. Factors predictive of response to interferon-alpha therapy in hepatitis C virus infection. *Hepatology* 1994; 19:1088–94.
6. Mizukoshi E, Kaneko S, Yanagi M, et al. Expression of interferon alpha/beta receptor in the liver of chronic hepatitis C patients. *J Med Virol* 1998; 56:217–23.
7. Ortaldo JR, Mantovani A, Hobbs D, Rubinstein M, Pestka S, Herberman RB. Effects of several species of human leukocyte interferon on cytotoxic activity of NK cells and monocytes. *Int J Cancer* 1983; 31: 285–9.
8. Tsubouchi E, Akbar SM, Horiike N, Onji M. Infection and dysfunction of circulating blood dendritic cells and their subsets in chronic hepatitis C virus infection. *J Gastroenterol* 2004; 39:754–62.
9. Popov S, Chenine AL, Gruber A, Li PL, Ruprecht RM. Long-term productive human immunodeficiency virus infection of CD1a-sorted myeloid dendritic cells. *J Virol* 2005; 79:602–8.
10. Schena M, Shalon D, Davis RW, Brown PO. Quantitative monitoring of gene expression patterns with a complementary DNA microarray. *Science* 1995; 270:467–70.
11. Schena M, Shalon D, Heller R, Chai A, Brown PO, Davis RW. Parallel human genome analysis: microarray-based expression monitoring of 1000 genes. *Proc Natl Acad Sci USA* 1996; 93:10614–9.
12. DeRisi J, Penland L, Brown PO, et al. Use of a cDNA microarray to analyse gene expression patterns in human cancer. *Nat Genet* 1996; 14:457–60.
13. Khan J, Simon R, Bittner M, et al. Gene expression profiling of alveolar rhabdomyosarcoma with cDNA microarrays. *Cancer Res* 1998; 58: 5009–13.
14. Iyer VR, Eisen MB, Ross DT, et al. The transcriptional program in the response of human fibroblasts to serum. *Science* 1999; 283:83–7.
15. Heller RA, Schena M, Chai A, et al. Discovery and analysis of inflammatory disease-related genes using cDNA microarrays. *Proc Natl Acad Sci USA* 1997; 94:2150–5.
16. Alizadeh AA, Eisen MB, Davis RE, et al. Distinct types of diffuse large B-cell lymphoma identified by gene expression profiling. *Nature* 2000; 403:503–11.
17. Desmet VJ, Gerber M, Hoofnagle JH, Manns M, Scheuer PJ. Classification of chronic hepatitis: diagnosis, grading and staging. *Hepatology* 1994; 19:1513–20.
18. Tanaka T, Tsukiyama-Kohara K, Yamaguchi K, et al. Significance of specific antibody assay for genotyping of hepatitis C virus. *Hepatology* 1994; 19:1347–53.
19. Kawai HE, Kaneko S, Honda M, Shirota Y, Kobayashi K. Alpha-feto-protein-producing hepatoma cell lines share common expression profiles of genes in various categories demonstrated by cDNA microarray analysis. *Hepatology* 2001; 33:676–91.
20. Honda M, Kaneko S, Kawai H, Shirota Y, Kobayashi K. Differential gene expression between chronic hepatitis B and C hepatic lesion. *Gastroenterology* 2001; 120:955–66.
21. Shirota Y, Kaneko S, Honda M, Kawai HE, Kobayashi K. Identification of differentially expressed genes in hepatocellular carcinoma with cDNA microarrays. *Hepatology* 2001; 33:832–40.
22. Honda M, Shimazaki T, Kaneko S. La protein is a potent regulator of replication of hepatitis C virus in patients with chronic hepatitis C through internal ribosomal entry site-directed translation. *Gastroenterology* 2005; 128:449–62.
23. Kawaguchi K, Honda M, Yamashita T, Shirota Y, Kaneko S. Differential gene alteration among hepatoma cell lines demonstrated by cDNA microarray-based comparative genomic hybridization. *Biochem Biophys Res Commun* 2005; 329:370–80.
24. Honda M, Kawai H, Shirota Y, Yamashita T, Kaneko S. Differential gene expression profiles in stage I primary biliary cirrhosis. *Am J Gastroenterol* 2005; 100:2019–30.
25. Honda M, Yamashita T, Ueda T, Takatori H, Nishino R, Kaneko S. Different signaling pathways in the livers of patients with chronic hepatitis B or chronic hepatitis C. *Hepatology* 2006; 44:1122–38.
26. Smith MW, Walters KA, Korth MJ, et al. Gene expression patterns that correlate with hepatitis C and early progression to fibrosis in liver transplant recipients. *Gastroenterology* 2006; 130:179–87.
27. Bigger CB, Guerra B, Brasky KM, et al. Intrahepatic gene expression during chronic hepatitis C virus infection in chimpanzees. *J Virol* 2004; 78:13779–92.
28. Ando T, Suguro M, Kobayashi T, Seto M, Honda H. Selection of casual gene sets for lymphoma prognostication from expression profiling and construction of prognostic fuzzy neural network models. *J Biosci Bioeng* 2003; 96:161–7.
29. Ando T, Suguro M, Kobayashi T, Seto M, Honda H. Multiple fuzzy neural network system for outcome prediction and classification of 220 lymphoma patients on the basis of molecular profiling. *Cancer Sci* 2003; 94:906–13.
30. Takahashi H, Kobayashi T, Honda H. Construction of robust prognostic predictors by using projective adaptive resonance theory as a gene filtering method. *Bioinformatics* 2005; 21:179–86.
31. Lempicki RA, Polis MA, Yang J, et al. Gene expression profiles in hepatitis C virus (HCV) and HIV coinfection: class prediction analyses before treatment predict the outcome of anti-HCV therapy among HIV-coinfected persons. *J Infect Dis* 2006; 193:1172–7.

q24

Clinical Studies

Liver International

DOI: 10.1111/j.1478-3231.2005.01231.x

The development and clinical features of splenic aneurysm associated with liver cirrhosis

Sunagozaka H, Tsuji H, Mizukoshi E, Arai K, Kagaya T, Yamashita T, Sakai A, Nakamoto Y, Honda M, Kaneko S. The development and clinical features of splenic aneurysm associated with liver cirrhosis.

Liver International 2006; 26: 291–297.

© 2006 The Author(s). Journal compilation © 2006 Blackwell Munksgaard

Abstract: *Objectives:* Splenic artery aneurysm (SAA) is usually asymptomatic, but can be fatal if it ruptures. Portal hypertensive patients with varix or splenomegaly are sometimes complicated by SAA. However, there have been no large-scale clinical studies regarding whether liver cirrhosis itself is associated with splenic aneurysm regardless of varix or splenomegaly. *Methods:* In the present study, we retrospectively analyzed 303 cirrhotic patients examined with arteriography. The diagnosis and characteristics of SAAs were determined, and the relation with splenic artery diameter was evaluated. *Results:* Nine patients (2.97%) had 12 complicated SAAs. The aneurysms, which measured 4–22 mm in diameter, were all saccular, and occurred commonly in the splenic hilum (50.0%). A correlation was noted between splenic artery diameter and aneurysm diameter ($R^2 = 0.706$). Aneurysm growth was strongly associated with an increase in diameter of the splenic artery trunk ($R^2 = 0.705$), which is closely related to arterial flow. *Conclusions:* SAA is considered a complication of cirrhosis. The increase in splenic artery diameter may result in SAA enlargement and rupture. Elective procedures should be considered based on the follow-up of main trunk or diameter of the splenic artery in addition to SAA size, a known risk factor of aneurysmal rupture.

Hajime Sunagozaka¹, Hirokazu Tsuji^{1,2}, Eishiro Mizukoshi¹, Kuniaki Arai¹, Takashi Kagaya¹, Tatsuya Yamashita¹, Akito Sakai¹, Yasunari Nakamoto¹, Masao Honda¹ and Shuichi Kaneko¹

¹Department of Gastroenterology, Graduate School of Medical Science, Kanazawa University, Ishikawa, Japan, ²Department of Gastroenterology, Kanazawa Municipal Hospital, Ishikawa, Japan

Key words: arteriography – liver cirrhosis – rupture – splenic aneurysm – splenic artery diameter

Shuichi Kaneko, Department of Gastroenterology, Graduate School of Medical Science, Kanazawa University, 13-1 Takara-machi, Kanazawa, Ishikawa 920-8641, Japan.
Tel: +81-76-265-2235
Fax: 81-76-234-4250
e-mail: skaneko@medf.m.kanazawa-u.ac.jp

Received 27 March 2005,
accepted 29 November 2005

Splenic artery aneurysm (SAA) is a disease that is usually asymptomatic but has a risk of rupture (1), and can be fatal because of hemorrhagic shock once it ruptures. As its first report in 1770 by Beaussier (2), SAA was thought to be a rare disease. However, recent advances in diagnostic imaging, such as celiac arteriography, Doppler ultrasound examination, and computed tomography (CT) scanning, have increased the chance of diagnosis (3). It has been reported that although the actual incidence of splenic aneurysm in autopsy cases is 0.05–1.6% (4), and it affects 7.1–50% of patients with portal hypertension, which is one of the risk factors in its development (3, 5, 6).

In patients with overt portal hypertension with varices, attention should be paid to the possibility of complication with SAA. However, not all cirrhotic patients have portal hypertensive features, such as gastro-esophageal varices or splenomegaly (7–9), and there have been no large-

scale clinical studies of whether cirrhosis itself is associated with SAA even if it is not a complication of portal hypertension. One cirrhotic patient in the present study with no varices actually suffered splenic aneurysmal rupture and died. The SAA development in chronic liver disease should be investigated in terms of the increasing incidence of liver cirrhosis worldwide. Therefore, we conducted a large-scale retrospective clinical study to determine the prevalence of SAA, the incidence of rupture, and its risk factors. In addition, we report the results of examinations along with the follow-up of some patients based on serial arteriography.

Patients and methods

Of the cirrhotic patients admitted to our hospital from January 1996 to May 2004, 303 consecutive patients underwent abdominal arteriography as part of a work up for hepatocellular carcinoma.

In the present study, the images of arteriography were reevaluated retrospectively to detect SAA. Informed consent for arteriography was obtained from each patient and the study protocol conformed to the ethical guidelines of the 1975 Declaration of Helsinki.

Cirrhosis was diagnosed histologically by liver biopsy in almost all patients, but was diagnosed clinically based on liver function tests and imaging findings if patients presented with potential contraindications for percutaneous liver biopsy, such as massive ascites or severe thrombocytopenia. Portal hypertension was estimated from the presence of varices, port-systemic shunts, or splenomegaly. The grade of esophageal varices (grades F0–3) was evaluated according to the classification described previously (10, 11). Splenic aneurysm was diagnosed with celiac arteriography. In patients complicated with SAA, the shape, location, and long diameter of aneurysms, and the maximum diameter of the main trunk of the splenic artery were evaluated. The locations of SAAs were defined as follows: intrasplenic area, splenic hilum, and dividing the main branch of the splenic artery into three equal parts (from the side of the celiac artery), the proximal area, the intermediate area, and the distal area of the splenic artery (12). Six patients with SAAs were examined by multiple arteriographies for 16–37 months (median 25.9). Therefore, the growth rate of SAA could be evaluated with regard to splenic artery diameter.

The possible associations were also investigated between SAA complication and patient

characteristics, such as age, gender, cause of cirrhosis, medical history, varices, and splenomegaly. The hepatic reserve and liver fibrosis were assessed from the Child–Pugh score, platelet count, prothrombin time, albumin level, type IV collagen (latex coagulation method), and indocyanine green clearance (ICG15R). The diagnosis and degree of splenomegaly were estimated by the spleen index (SI: the product of the long axis multiplied by the short axis of the spleen, measured from the splenic hilum) based on abdominal ultrasound (Table 1).

The patient who died of hemorrhagic shock following splenic aneurysmal rupture was autopsied. Slides were prepared from tissue samples, which were fixed in 10% buffered formalin, and then examined with hematoxylin–eosin, Elastic van Gieson, and silver staining.

The data are given as means \pm standard deviation. The differences in patient characteristics between the SAA and non-SAA (control) groups were tested by the chi-square test, Mann–Whitney *U*-test, and two test.

Results

Incidence of splenic arterial aneurysm

The cirrhotic patients ($n = 303$) consisted of 208 men and 95 women, and had a mean age of 66.3 ± 7.4 years. The cause of cirrhosis was viral hepatitis, particularly hepatitis C virus (HCV), in approximately 75% of the patients. The results of liver function tests were consistent with cirrhosis:

Table 1. Clinical features of patients

	Control group	SAA group
Number	294	9
Age (years)	66.5 ± 7.3	64.3 ± 11.1
Sex (male:female)	205:89	3:6
Etiology		
HBV	45	1
HCV	208	7
HBV+HCV	4	0
Alcohol	24	1
HCV+alcohol	3	0
PBC	10	0
Hematologic characteristics		
Platelet ($\times 10^3/\mu\text{l}$)	97.7 ± 48.9	101.0 ± 50.1
Prothrombin time (%)	65.0 ± 16.4	61.2 ± 12.4
Albumin (g/dl)	3.7 ± 0.7	3.7 ± 0.7
Type IV collagen (ng/ml)	270.1 ± 144.9	269.4 ± 160.1
ICG15R (%)	26.0 ± 14.2 ($n = 261$)	28.4 ± 13.9 ($n = 7$)
Splenoindex (cm^2)	29.2 ± 14.1 ($n = 228$)	25.8 ± 9.4
Child–Pugh score	6.5 ± 1.3	6.2 ± 1.1
Complicated varix	54.4% (160/294)	44.4% (4/9)

Data are given as mean \pm SD, there are no data with $P < 0.05$. SAA, splenic artery aneurysm; HBV, hepatitis B virus; HCV, hepatitis C virus; PBC, primary biliary cirrhosis.

decreases in platelet count, prothrombin time result, and albumin level; increases in ICG15R value and type IV collagen; and varices (Table 1).

Nine of all the patients were complicated with SAA, and had an average age of 64.3 ± 11.1 years at the time of diagnosis, which was not significantly different from the non-complicated patients. The Child-Pugh score for the nine patients with SAA averaged 6.2 ± 1.1 . Of the nine patients with SAA, three were men and six were women, indicating sex-specific difference ($P = 0.020$). Two of the six women had a history of three or more pregnancies. Hepatitis B virus, HCV, and alcoholic liver disease caused cirrhosis in one, seven and one of the patients with SAA, respectively. There were no significant differences in platelet count, prothrombin test result, albumin level, type IV collagen level, ICG15R value, esophageal varices, or SI between the patients with and without SAA (Table 1).

Characteristics of splenic artery aneurysm

Nine patients had a total of 12 SAAs, which were not complicated by calcification or thrombi. Multiple SAAs (up to three) were observed in two patients. The SAAs ranged in diameter from 4 to 22 mm (mean 14.1 mm), and were saccular regardless of size or location. No fusiform SAA was observed. One SAA was located in each of the proximal (8.3%), intermediate (8.3%), and distal (8.3%) segments; six SAAs (50.0%) in the splenic hilum; and three SAAs (25.0%) within the spleen (Table 2). One hundred and sixty (54.4%) of the 294 patients without SAA, and four (44.4%) of the nine patients with SAA were complicated with esophageal varices. Moreover, 171 (58.1%) of the 294 patients without SAA, and eight (88.9%) of the nine patients with SAA were complicated with splenomegaly. However,

there were no significant differences in the degree of SI between the patients with and without SAA ($P = 0.781$) (Table 1).

Splenic artery aneurysm and splenic artery

The splenic hyperkinetic state is associated with the development of SAA (5, 6, 13–16). As shown in Fig. 1, we observed a correlation between the diameter of the main trunk of the splenic artery and the size of complicating SAA ($R^2 = 0.706$). In addition, we confirmed the serial changes in eight SAAs occurring over long periods in six patients by celiac arteriography, which was performed to examine hepatocellular carcinoma. During the 16–37 months of follow-up (median 25.9), the diameter of the main trunk of the splenic artery and the long diameter of the SAAs increased by 0.18 and 2.65 mm on average, respectively (Fig. 2). Time-lapse observations indicated that the SAA diameter remained unchanged in some patients, but increased in others, such as Case No. 5 shown in Fig. 3. The increase in main trunk of the splenic artery rather than the main trunk diameter itself, contributed to the increase in SAA diameter ($R^2 = 0.705$) (Fig. 4).

Analysis of ruptured SAA

One patient with SAA (Case No. 1) died of hemorrhagic shock because of rupture (Table 2). Autopsy revealed an irregular internal elastic lamina of the ruptured aneurysm wall with vacuolar degeneration and thinning of the tunica media. As the defects of the intima, tunica media, and adventitia corresponded to a massive subserosal hematoma, the cause of death was diagnosed as SAA rupture. Another noteworthy lesion was an organized thrombus that was located in the splenic vein and extended to the main trunk of the

Table 2. Clinical features of patients with splenic aneurysm

Case no.	Age	Sex	Etiology	Splenic aneurysm			Main trunk of splenic artery (mm)	Splenoindex (cm ²)	Esophageal varix	Remark
				Number	Location	Size (mm)				
1	55	M	HCV	2	H	22.0	8.4	7.6 × 6.2	(–)	Ruptured
					M	10.0				
2	71	F	HCV	1	I	4.6	3.8	4.9 × 4.5	(–)	
3	80	M	Alcohol	1	H	12.0	5.0	5.1 × 4.7	F1	
4	62	F	HCV	1	I	6.0	5.0	5.5 × 4.5	(–)	
5	63	F	HCV	1	H	18.0	4.8	5.5 × 4.6	F2	3 pregnancies
6	73	F	HCV	3	H	22.0	5.0	4.9 × 4.9	F1	
					P	20.0				
					D	15.0				
7	44	F	HCV	1	H	18.0	6.0	5.7 × 5.1	(–)	4 pregnancies
8	58	M	HCV	1	I	4.0	4.0	6.0 × 4.2	F0	
9	73	F	HBV	1	H	15.0	5.8	3.6 × 3.0	(–)	

Location: P, proximal; M, intermediate; D, distal; H, hilum; I, intrasplenic; M, male; F, female; HCV, hepatitis C virus; HBV, hepatitis B virus.

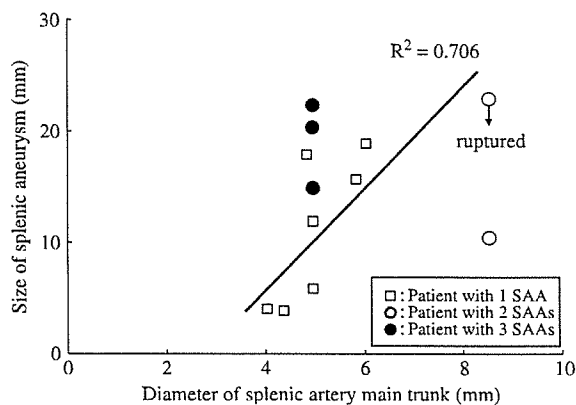


Fig. 1. Correlation between splenic artery diameter and size of splenic artery aneurysm (SAA). Open and closed circles represented the patients with two and three SAAs, respectively. Open squares represented the patients with one SAA. We observed a correlation between the diameter of the main trunk of the splenic artery and the size of complicating SAA ($R^2 = 0.706$).

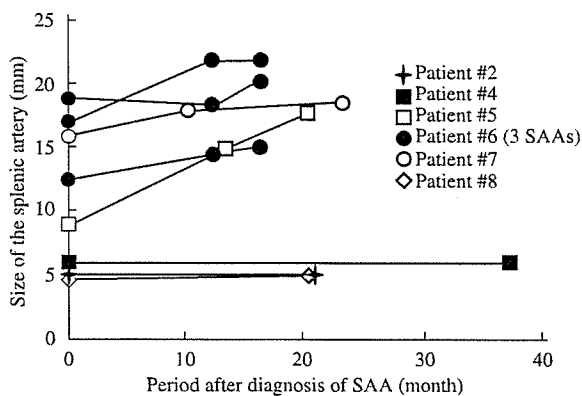


Fig. 2. Sequential changes of splenic artery aneurysms (SAAs). The sizes of eight SAAs in six patients were measured sequentially by celiac arteriography during a mean follow-up period of 25.9 months. The diameter of the main trunk of the splenic artery and the long diameter of the SAAs increased by 0.18 and 2.65 mm on an average, respectively. Note that some SAAs became enlarged, while the sizes of others remained unchanged.

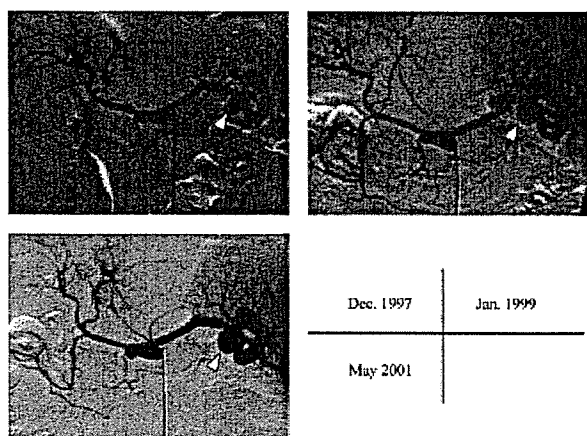


Fig. 3. Sequential changes of splenic artery aneurysm (SAA) on celiac arteriography. Arrowheads indicate the SAA, and its diameter was shown to have increased (Case No. 5).

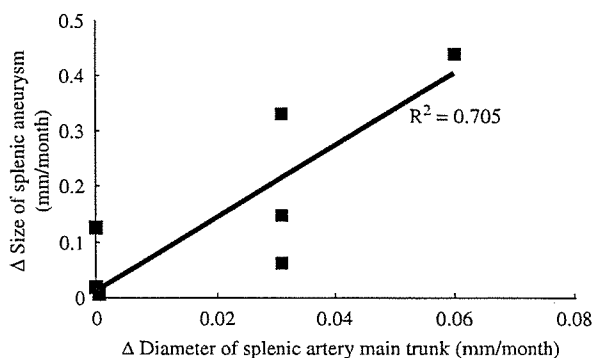


Fig. 4. Correlations between the growth rate of splenic artery diameter and size of splenic artery aneurysm. The tendency of the main trunk of the splenic artery to increase, that is, the tendency of splenic blood flow to increase contributed to the elevation in the splenic aneurysm diameter.

portal vein, but had not been detected by imaging 4 months before death (Fig. 5).

Discussion

SAA clinical presentation and characteristics in liver cirrhosis

The incidence of SAA varies widely depending on the subjects studied, and has been reported to be 0.05–1.6% in general autopsies (4). Multiple risk factors for the formation of SAAs have been reported (17, 18), and the high-risk group should be followed up carefully or given preventive therapy because SAA rupture is associated with a high mortality rate. The actual incidence of SAA in portal hypertensive patients diagnosed by the presence of esophageal and gastric varices has been reported to be 7.1–50% (3, 5, 6, 13, 16, 19), which is higher than that in the general population. However, previous studies were designed to detect only patients with varices. Although varices are a frequent sign of portal hypertension, the prevalence is only 44–51% (20, 21). Moreover, patients without varices, such as Case No. 1, could present aneurysmal rupture, suggesting that hemodynamics in liver cirrhosis should be considered risk factors of rupture. The present study was the first to analyze SAA in cirrhotic patients regardless of portal hypertensive signs, such as varices. With recent advances in technology, celiac arteriography is now used to examine hepatocellular carcinoma in cirrhotic patients to predict the stage of disease and to determine treatment management (22, 23). Angiography remains the gold standard to localize the lesions and determine the presence of SAA (24), and retrospective estimation of arteriography can allow the detection of incidental splenic aneurysm.

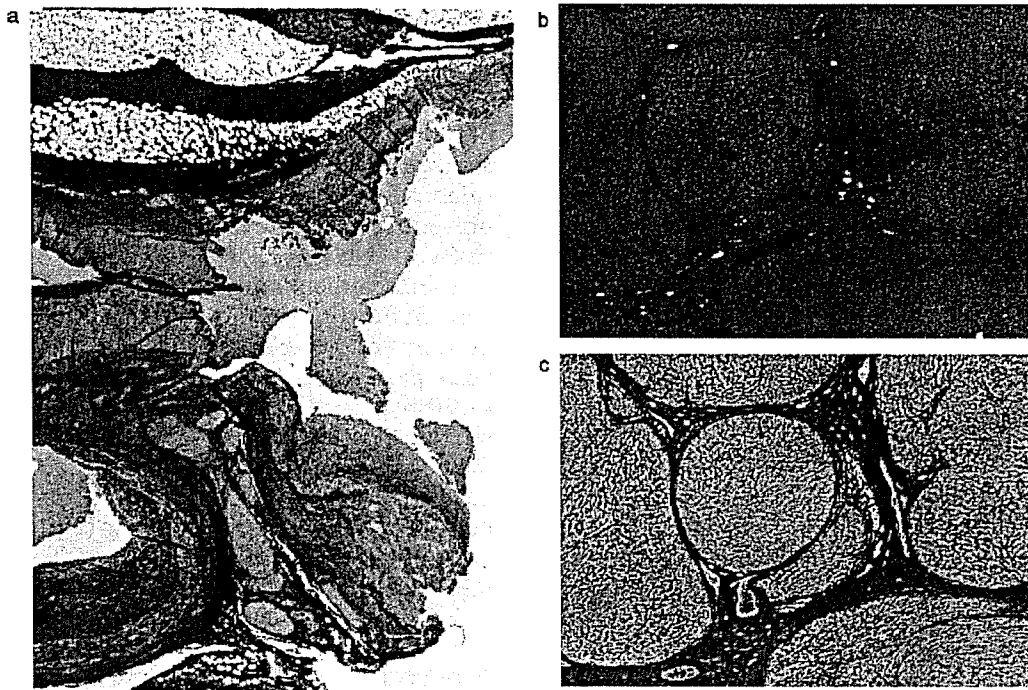


Fig. 5. Histopathological examination of ruptured aneurysm and cirrhotic liver tissue. (a) The ruptured aneurysm showing an irregular internal elastic lamina and vacuolar degeneration and thinning of the tunica media. The defects of the intima, tunica media, and adventitia corresponded with a massive subserosal hematoma (arrow). (Elastic van Gieson stain, $\times 4$). (b, c) The hepatic parenchyma displayed fibrosis and nodule formation of varying sizes, implying liver cirrhosis. (b) Hematoxylin-eosin stain, $\times 32$; (c) Silver stain, $\times 32$).

In the present study, complicating gastroesophageal varices and splenomegaly ($SI > 20$) were observed in 54.1% (164/303) and 59.1% (179/303) of the cirrhotic patients analyzed, respectively, i.e., in about half of the patients. Nine (2.97%) of the 303 cirrhotic patients had SAA. All nine cases were diagnosed histologically as liver cirrhosis. Four of 164 patients with varices (2.4%) and five of the 139 patients without varices (3.6%) had SAA. Thus, we could not determine the risk of SAA based solely on the presence of varices. Moreover, the size of the spleen (SI) in SAA patients was not significantly different from that in the non-SAA patients ($P = 0.781$). Although the incidence of SAA in the present study was lower than that in patients with varices reported previously (3, 5, 6, 25), it was about 1.9–59.4-fold higher than the incidence reported in autopsy cases where no patient characteristics were defined (4). The lower prevalence may have been because angiography was only used to examine patients with at least one episode of varix bleeding or advances in image analysis allowed us to distinguish early cirrhosis from chronic hepatitis although liver cirrhosis was finally diagnosed by liver biopsy. These findings suggested a need to regard not only varices but also cirrhosis itself as associated factors for SAA.

Cirrhotic patients undergoing arteriography should be evaluated for not only intrahepatic malignancy (22, 23) but also for SAA.

Mechanism for development of SAA

In the present study, we evaluated the location, size, and changes in size of SAAs accurately by serial arteriography. The ruptured aneurysm in the present study measured 22 mm. A previous report suggested that the risk of rupture might be linked to size (18), which is associated with splenic artery flow (6, 13). Arterial blood flow has been clearly shown to be related to arterial diameter (26). The question arises whether the size of SAA is correlated with the diameter of the splenic artery. In the present study, we found a relationship between SAA diameter and the main trunk of the splenic arteries as shown in Fig. 1. Cirrhosis-associated changes in hemodynamics systemically result in increased cardiac output, increased vascular contents, and portal congestion with outflow impairment. Then, the hemodynamic changes impose stress on the vascular wall of the portal vein with resultant primary alterations in wall structure, leading to local vascular dilation and splenic aneurysm formation (5, 14–16, 27). We consider that in the splenic

artery, the increase in splenic artery blood flow is closely related to the growth of SAA.

In addition, we have followed SAAs over long periods by abdominal arteriography, and our results have indicated that some SAAs became enlarged, while others did not change in size, as shown in Fig. 2. The most rapid growth rate was 9 mm over 20 months. Notably, not a longer follow-up period but an increase in the diameter of the splenic artery was associated with faster enlargement of SAAs. The increase in splenic artery diameter was also thought to be essential for the growth of the SAA.

Risk of rupture and management of SAA

SAA rupture is accompanied by massive intra-peritoneal hemorrhage leading rapidly to hemorrhagic shock and poor prognosis. Boijssen and Efsing (13) and Spittel et al. (28) reported rupture frequencies of 6% and 8.2%, respectively. Berger et al. (29) reported that the frequency of rupture secondary to portal hypertension was 35%. Although hemostatic procedures, such as open abdominal splenic aneurysm ligation and splenectomy, and transcatheter embolization are indicated for the treatment of splenic aneurysmal rupture (30–32), the prognosis remains poor. Lee et al. (19) reported a mortality rate of 17% after SAA rupture in patients with no portal hypertension complication, whereas portal hypertensive patients had a significantly poorer prognosis with a mortality rate of 57%. They also reported that 84% of patients undergoing elective procedures survived after a mean follow-up period of 46 months. Therefore, identification of risk factors for SAA rupture and appropriate preventive measures are more important than treatment after rupture.

Risk factors for rupture included no encapsulation (calcification), aneurysm size, and a tendency toward enlargement, clinical symptoms, and pregnancy (17). It has been reported that aneurysms less than 15 mm in diameter have a low risk of rupture, making them amenable to conservative follow-up (33), whereas about 3–10% of aneurysms more than 20 mm in diameter rupture (3, 13, 17, 34). In the present study, two patients had a total of three aneurysms more than 20 mm in maximum long diameter, one of which ruptured. None of the five aneurysms less than 15 mm in diameter ruptured. Although the size of SAA is a significant risk factor, the splenic artery flow related to the diameter of the splenic artery should be measured to estimate the risk. The patient who died of rupture in the present study had portal thrombosis, which was confirmed at

autopsy but had not been diagnosed by imaging 4 months before death. We speculate that rapid thrombus formation resulted in a rapid increase in splenic artery pressure secondary to stagnation of blood flow in the spleen, leading to growth and rupture of the fragile aneurysm. In cases in which splenic flow is increasing, it is necessary to take preventive procedures and to treat them aggressively.

The treatment option is limited by impaired hepatic function. Although open combined resection of the splenic artery and spleen has generally been performed (19), less-invasive laparoscopic surgical procedures are now possible depending on the location and number of SAAs (35, 36). Partial splenic embolization could be used as an alternative procedure dependent on our study because it decreases splenic flow (37) resulting in prevention of aneurysmal rupture. To determine the indication for treatment, celiac arteriography has the highest sensitivity for the diagnosis and measurement of SAA (31). However, this procedure is too invasive for follow-up. Therefore, a few studies have reported that less-invasive Doppler ultrasound was useful for assessment of the size of SAAs and the amount of splenic arterial blood flow (27, 38). Elective measures could be considered in patients with SAA if increase in aneurysmal size or splenic artery diameter are observed.

Conclusions

The incidence of SAA in cirrhotic patients is 2.97%, and about 1.9–59.4-fold higher than that of the general population. The increase in main trunk of the splenic artery, i.e., the increase of splenic blood flow, rather than the main trunk diameter itself, contributed to the increase in SAA diameter. SAA is considered to be a complication of cirrhosis. Increases in splenic artery diameter contribute to the progression and rupture of the SAA. Elective procedures should be considered for high-risk groups.

References

1. STANLEY J C, WAKEFIELD T W, GRAHAM L M, WHITEHOUSE W M Jr., ZELENOCK G B, LINDENAUER S M. Clinical importance and management of splanchnic artery aneurysms. *J Vasc Surg* 1986; 3: 836–40.
2. BEAUSSIER M. Sur un aneurysme de l'artere splenique: dont les parois se sont ossifiees. *J Med Clin Pharmacol Paris* 1770; 32: 157.
3. STANLEY J C, FRY W J. Pathogenesis and clinical significance of splenic artery aneurysms. *Surgery* 1974; 76: 898–909.
4. MOORE S W, GUIDA P M, SCHUMACHER H W. Splenic artery aneurysm. *Bull Soc Int Chir* 1970; 29: 210–8.

5. MANENTI A, WILLIAMS R. Injection studies of the splenic vasculature in portal hypertension. *Gut* 1966; 7: 175-80.
6. PUTTINI M, ASENI P, BRAMBILLA G, BELLI L. Splenic artery aneurysms in portal hypertension. *J Cardiovasc Surg (Torino)* 1982; 23: 490-3.
7. SARIN S K, LAHOTI D, SAXENA S P, MURTHY N S, MAKWANA U K. Prevalence, classification and natural history of gastric varices: a long-term follow-up study in 568 portal hypertension patients. *Hepatology* 1992; 16: 1343-9.
8. DE FRANCHIS R, PRIMIGNANI M. Natural history of portal hypertension in patients with cirrhosis. *Clin Liver Dis* 2001; 5: 645-63.
9. MERLI M, NICOLINI G, ANGELONI S, et al. Incidence and natural history of small esophageal varices in cirrhotic patients. *J Hepatol* 2003; 38: 266-72.
10. JAPANESE RESEARCH SOCIETY FOR PORTAL HYPERTENSION. The general rules for recording endoscopic findings on esophageal varices. *Jpn J Surg* 1980; 10: 84-7.
11. THE NORTH ITALIAN ENDOSCOPIC CLUB FOR THE STUDY AND TREATMENT OF ESOPHAGEAL VARICES. Prediction of the first variceal hemorrhage in patients with cirrhosis of the liver and esophageal varices. A prospective multicenter study. *The North Italian Endoscopic Club for the Study and Treatment of Esophageal Varices. N Engl J Med* 1988; 319: 983-9.
12. OHTA M, HASHIZUME M, UENO K, TANOUE K, SUGIMACHI K, HASUO K. Hemodynamic study of splenic artery aneurysm in portal hypertension. *Hepatogastroenterology* 1994; 41: 181-4.
13. BOIJSEN E, EFSING H O. Aneurysm of the splenic artery. *Acta Radiol Diagn (Stockholm)* 1969; 8: 29-41.
14. FEIST J H, GAJARAJ A. Extra- and intrasplenic artery aneurysms in portal hypertension. *Radiology* 1977; 125: 331-4.
15. SCHEININ T M, VANTTINEN E. Aneurysms of the splenic artery in portal hypertension. *Ann Clin Res* 1969; 1: 165-8.
16. OHTA M, HASHIZUME M, TANOUE K, KITANO S, SUGIMACHI K, YASUMORI K. Splenic hyperkinetic state and splenic artery aneurysm in portal hypertension. *Hepatogastroenterology* 1992; 39: 529-32.
17. TRASTEK V F, PAIROLERO P C, BERNATZ P E. Splenic artery aneurysms. *World J Surg* 1985; 9: 378-83.
18. ABBAS M A, STONE W M, FOWL R J, et al. Splenic artery aneurysms: two decades experience at Mayo clinic. *Ann Vasc Surg* 2002; 16: 442-9.
19. LEE P C, RHEE R Y, GORDON R Y, FUNG J J, WEBSTER M W. Management of splenic artery aneurysms: the significance of portal and essential hypertension. *J Am Coll Surg* 1999; 189: 483-90.
20. SCHEPIS F, CAMMA C, NICEFORO D, et al. Which patients with cirrhosis should undergo endoscopic screening for esophageal varices detection? *Hepatology* 2001; 33: 333-8.
21. MADHOTRA R, MULCAHY H E, WILLNER I, REUBEN A. Prediction of esophageal varices in patients with cirrhosis. *J Clin Gastroenterol* 2002; 34: 81-5.
22. HAYASHI M, MATSUI O, UEDA K, et al. Correlation between the blood supply and grade of malignancy of hepatocellular nodules associated with liver cirrhosis: evaluation by CT during intraarterial injection of contrast medium. *Am J Roentgenol* 1999; 172: 969-76.
23. HAYASHI M, MATSUI O, UEDA K, KAWAMORI Y, GABATA T, KADOYA M. Progression to hypervascular hepatocellular carcinoma: correlation with intranodular blood supply evaluated with CT during intraarterial injection of contrast material. *Radiology* 2002; 225: 143-9.
24. DAVE S P, REIS E D, HOSSAIN A, TAUB P J, KERSTEIN M D, HOLLIER L H. Splenic artery aneurysm in the 1990s. *Ann Vasc Surg* 2000; 14: 223-9.
25. DE VRIES J E, SCHATTEKERK M E, MALT R A. Complications of splenic artery aneurysm other than intraperitoneal rupture. *Surgery* 1982; 91: 200-4.
26. SUWA N, NIWA T, FUKASAWA H, SASAKI Y. Estimation of intravascular blood pressure gradient by mathematical analysis of arterial casts. *Tohoku J Exp Med* 1963; 79: 168-9.
27. NISHIDA O, MORIYASU F, NAKAMURA T, et al. Hemodynamics of splenic artery aneurysm. *Gastroenterology* 1986; 90: 1042-6.
28. SPITTEL J J, FAIRBAIRN J F, KINCAID O W, REMINE W H. Aneurysm of the splenic artery. *J Am Med Assoc* 1961; 75: 452.
29. BERGER K, FORSEE J H, FURST J N. Splenic arterial aneurysm. *Ann Surg* 1953; 137: 108.
30. CAILLOUETTE J C, MERCHANT E B. Ruptured splenic artery aneurysm in pregnancy. Twelfth reported case with maternal and fetal survival. *Am J Obstet Gynecol* 1993; 168: 1810-1, discussion 1811-3.
31. YEH T S, JAN Y Y, JENG L B, HWANG T L, WANG C S, CHEN M F. Massive extra-enteric gastrointestinal hemorrhage secondary to splanchnic artery aneurysms. *Hepatogastroenterology* 1997; 44: 1152-6.
32. DE PERROT M, BUHLER L, DELEVAL J, BORISCH B, MENTHA G, MOREL P. Management of true aneurysms of the splenic artery. *Am J Surg* 1998; 175: 466-8.
33. AYALON A, WIESNER R H, PERKINS J D, TOMINAGA S, HAYES D H, KROM R A. Splenic artery aneurysms in liver transplant patients. *Transplantation* 1988; 45: 386-9.
34. BUSUTTIL R W, BRIN B J. The diagnosis and management of visceral artery aneurysms. *Surgery* 1980; 88: 619-24.
35. TARAZOV P G, PROZOROVSKII K V. Embolization of the hepatic artery in a spontaneous intrahepatic arterioportal fistula. *Vestn Rentgenol Radiol* 1991; 86-8.
36. HASHIZUME M, OHTA M, UENO K, OKADOME K, SUGIMACHI K. Laparoscopic ligation of splenic artery aneurysm. *Surgery* 1993; 113: 352-4.
37. MUKAIYA M, HIRATA K, YAMASHIRO K, KATSURAMAKI T, KIMURA H, DENNO R. Changes in portal hemodynamics and hepatic function after partial splenic embolization (PSE) and percutaneous transhepatic obliteration (PTO). *Cancer Chemother Pharmacol* 1994; 33(Suppl.): S37-41.
38. OSAWA M, MASUI M, WAKASUGI C. Rupture of a giant splenic artery aneurysm: report of an autopsy case. *Am J Forensic Med Pathol* 1991; 12: 337-9.

Diverse Effects of Cyclosporine on Hepatitis C Virus Strain Replication

Naoto Ishii,¹† Koichi Watashi,¹† Takayuki Hishiki,¹ Kaku Goto,¹ Daisuke Inoue,¹ Makoto Hijikata,¹ Takaji Wakita,² Nobuyuki Kato,³ and Kunitada Shimotohno^{1*}

Laboratory of Human Tumor Viruses, Department of Viral Oncology, Institute for Virus Research, Kyoto University, Kyoto,¹ Department of Microbiology, Tokyo Metropolitan Institute for Neuroscience, Tokyo,² and Department of Molecular Biology, Okayama University Graduate School of Medicine, Dentistry and Pharmaceutical Sciences, Okayama,³ Japan

Received 18 December 2005/Accepted 10 February 2006

Recently, a production system for infectious particles of hepatitis C virus (HCV) utilizing the genotype 2a JFH1 strain has been developed. This strain has a high capacity for replication in the cells. Cyclosporine (CsA) has a suppressive effect on HCV replication. In this report, we characterize the anti-HCV effect of CsA. We observe that the presence of viral structural proteins does not influence the anti-HCV activity of CsA. Among HCV strains, the replication of genotype 1b replicons was strongly suppressed by treatment with CsA. In contrast, JFH1 replication was less sensitive to CsA and its analog, NIM811. Replication of JFH1 did not require the cellular replication cofactor, cyclophilin B (CyPB). CyPB stimulated the RNA binding activity of NS5B in the genotype 1b replicon but not the genotype 2a JFH1 strain. These findings provide an insight into the mechanisms of diversity governing virus-cell interactions and in the sensitivity of these strains to antiviral agents.

Hepatitis C virus (HCV), a member of the *Flaviviridae* family, has a positive-strand RNA genome (1, 26). The genome encodes a large precursor polyprotein, which is cleaved by host and viral proteases to generate at least 10 functional viral proteins: core, envelope 1 (E1), E2, p7, nonstructural protein 2 (NS2), NS3, NS4A, NS4B, NS5A, and NS5B (6, 8). NS5B is an RNA-dependent RNA polymerase that is crucial for viral genome replication (1, 26). There is genetic heterogeneity within the HCV genome. Currently, these differences are classified into six genotypes that are further segregated into a series of subtypes (4, 23). In Japan, genotype 1b is predominant; roughly 65% of cases of HCV-related chronic hepatitis involve genotype 1b. By comparison, genotype 2a is present in 17% of these patients (13, 23).

Sustained infection of HCV is the major cause of chronic liver diseases such as chronic hepatitis, liver cirrhosis, and hepatocellular carcinoma (16). Rarely, HCV causes fulminant hepatitis (13). The predominant treatment for HCV-infected patients is interferon (IFN) or polyethylene glycol-conjugated IFN alone or in combination with ribavirin (19, 20). However, alternative anti-HCV therapies are needed because virus is not eliminated in about half of the treated patients (19, 20). Lohmann et al. have developed the HCV subgenomic replicon system, in which an HCV subgenomic replicon autonomously replicates in Huh-7 cells (HCV replicon cells) (18). This replicon comprises the HCV 5' untranslated region (5'UTR) containing an internal ribosomal entry site (IRES), the neomycin phosphotransferase gene, the encephalomyocarditis virus (EMCV) IRES, the coding region for HCV NS3 through NS5B, and the HCV

3'UTR (subgenomic replicon), but it lacks the coding region for the core and envelope proteins, as well as p7 and NS2 (Fig. 1). Subsequently, a genome-length (full-genome) replicon has been developed. This construct contains a full-genome length of HCV, including the coding regions for the core protein through NS2 (Fig. 1) (5, 10). We can evaluate HCV replication using these subgenomic or genome-length replicon systems. Previously, we established HCV subgenomic replicon cells carrying HCV genotype 1b NN strain (15, 29). We demonstrated that an immunosuppressant, cyclosporine (CsA), has anti-HCV activity in these cells (29). In addition, we determined the molecular mechanism of the anti-HCV effect of CsA on this replicon; cyclophilin B (CyPB), one of the cellular targets of CsA, is a cellular replication cofactor of the HCV genome (31). CyPB interacts with NS5B to promote its RNA binding activity (for a detailed description, see reference 31). CsA is suggested to suppress HCV genome replication by inhibiting the functional association of CyPB with NS5B. Another group also reported anti-HCV function of CsA using a subgenomic replicon of other genotype 1b strain, HCV-N (22). In this study, we demonstrate that CsA also has a strong anti-HCV activity in other available genotype 1b replicons carrying the Con1 and O strains (12, 18).

Recently, Wakita and colleagues reported that a replicon of HCV genotype 2a JFH-1 strain, which was isolated from a case of type-C fulminant hepatitis, has a much stronger level of replication activity than genotype 1b replicons in Huh-7 cells (13, 27). A production system of infectious viral particles was recently established with this high-replication-competent strain (17, 27, 34). This viral strain may acquire a growth advantage compared with many other strains, although the underlying mechanism is unknown. In this study, we described a characteristic difference in the replication of JFH1 compared to that of genotype 1b replicons.

Here, we report that JFH1 replication is less sensitive to CsA than genotype 1b strains, although the interaction of

* Corresponding author. Mailing address: Laboratory of Human Tumor Viruses, Department of Viral Oncology, Institute for Virus Research, Kyoto University, 53 Kawaharacho, Shogoin, Sakyo-ku, Kyoto 606-8507, Japan. Phone: 81-75-751-4000. Fax: 81-75-751-3998. E-mail: kshimoto@virus.kyoto-u.ac.jp.

† N.I. and K.W. contributed equally to this work.

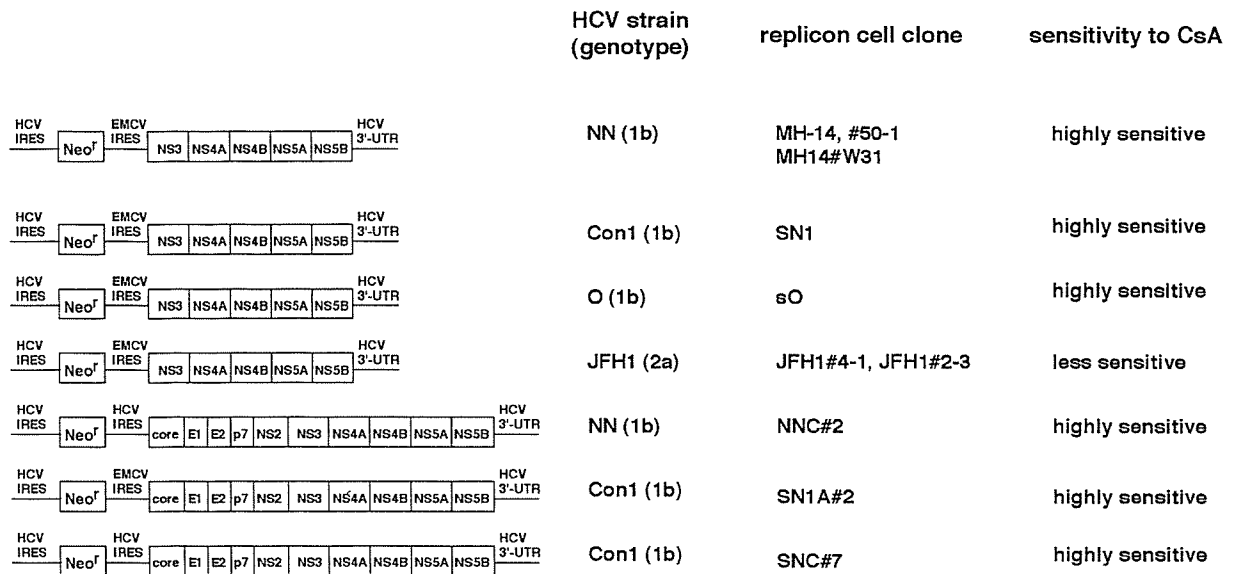


FIG. 1. Schematic representation of the constructs of HCV subgenomic and genome-length replicon RNA. On the left, the constructs of each replicon RNA are shown. HCV strains, as well as genotypes from which the replicon RNA sequences are derived, are indicated in the second column. The names of replicon cell clones established with each replicon RNA are in the third column. The sensitivity to CsA of each replicon RNA revealed in this study is summarized in the fourth column. The replicon RNAs comprise the HCV 5'UTR, including HCV IRES, the neomycin phosphotransferase gene (*Neo^r*), EMCV IRES, or HCV IRES, the coding region for HCV proteins NS3 to NS5B (subgenomic) or core to NS5B (genome length or full genome), and HCV 3'UTR. MH-14 (NN/1b/SG), #50-1 (NN/1b/SG), MH14#W31 (NN/1b/SG), SN1 (Con1/1b/SG), sO (O/1b/SG), JFH1#4-1 (JFH1/2a/SG), and JFH1#2-3 (JFH1/2a/SG) cells carry subgenomic replicons, while NNC#2 (NN/1b/FL), SN1A#2 (Con1/1b/FL), and SNC#7 (Con1/1b/FL) cells have genome-length replicons. NNC#2 (NN/1b/FL) and SNC#7 (Con1/1b/FL) cells contain the replicon RNA without EMCV IRES.

CyPB with NS5B is observed with this replicon. However, genome replication and RNA binding activity of NS5B are independent of CyPB. We have exploited a chemical compound to demonstrate how strain diversity can be generated by underlying differences in the mechanisms of the virus-cell interaction. These findings provide important insight into the mechanisms that mediate the efficacy of antiviral agents.

MATERIALS AND METHODS

Cell culture. Huh-7 cells were cultured in Dulbecco's modified Eagle medium (Invitrogen) with 10% fetal bovine serum, nonessential amino acids (Invitrogen), and L-glutamine (Invitrogen). MH-14, #50-1, MH14#W31, SN1, sO (formerly named 1B2R1), JFH1#4-1, and JFH1#2-3 cells (12, 13, 15, 18, 29), carrying subgenomic replicons, and NNC#2, SN1A#2, and SNC#7 cells, carrying full-genome replicons, were cultured in the above medium supplemented with 300- to 500- μ g/ml G418 (Invitrogen). In the assay measuring the response to CsA, NIM811, or PSC833 (Fig. 2, 3, and 4), we seeded small numbers of each replicon cells (7×10^3 to 15×10^3 cells/12-well plate) and treated with each drug. Culture medium was changed every 3 days (CsA, NIM811, or PSC833 was supplemented in the fresh medium for the treatment groups). We did not perform any passages in the assay period. At day 7, the cells were 70 to 90% confluent. A schematic representation of the constructs of HCV replicon RNAs, the name of HCV strains from which the replicon RNA sequences are derived, and the name of replicon cell clones used in this study are summarized in Fig. 1. Since many replicon clones were used in this study, we list "strain/genotype/length of the replicon construct" in parentheses after the names of each cell clone in Results and in the figure legends to avoid confusion between names; for example, MH-14 (NN/1b/SG), JFH1#4-1 (JFH1/2a/SG), and SN1A#2 (Con1/1b/FL) cells. The designations SG and FL indicate subgenomic and full-genome replicons, respectively.

Establishment of replicon cells. MH-14, #50-1, sO, JFH1#4-1, and JFH1#2-3 cells were described previously (12, 13, 15, 29). The replicon RNAs were produced using a MEGAscript T7 kit (Ambion) from pMH14, pSN1, pNNC, pSN1A, and pSNC plasmids for the establishment of the MH14#W31, SN1,

NNC#2, SN1A#2, and SNC#7 replicon cells, respectively. For the establishment of MH14#W31, we transfected RNA into the Huh-7 cell strain which was identical to the parental cells of JFH1#4-1 and JFH1#2-3. Each replicon RNA was transfected into Huh-7 cells, following the selection with the medium in the presence of 500- to 1,000- μ g/ml G418 for around 4 weeks. The resultant cell colonies were isolated and expanded. The HCV RNA titers in cell clones carrying JFH1 replicons were not significantly different from those in established cell clones carrying genotype 1b replicons.

Plasmid construction. pSN1, the sequence of which is derived from I377NS3-3' (18), was prepared essentially as described previously (15). pSN1A was generated by inserting the region from the core to NS2 of pM1LE (15) into the upstream coding region for NS3 in pSN1. To obtain pSNC, the EMCV IRES of pSN1A was replaced by the HCV IRES. pNNC was produced by inserting the coding region from NS3 to NS5B of pM1LE into pSNC.

Real-time reverse transcription-PCR (RT-PCR) analysis. The 5'UTR of HCV genome RNA was quantified using the ABI PRISM 7700 sequence detector (Applied Biosystems) as described previously (29).

Immunoblot analysis. Immunoblot analysis was performed as described previously (30). The primary antibodies used in this study were anti-core, anti-E2 (kindly provided by M. Kohara, Tokyo Metropolitan Institute of Medical Science), anti-NS3, anti-NS5A (a generous gift from A. Takamizawa, Osaka University), anti-NS5B (NS5B-6; kindly provided by I. Fukuya, Osaka University), anti-CyPA (Upstate Cell Signaling), anti-CyPB (Affinity BioReagents), and anti-tubulin (Oncogene).

Immunoprecipitation assay and RNA-protein binding precipitation assay. Immunoprecipitation and RNA-protein binding precipitation were performed as described previously (30, 31).

RNA interference technique. The condition of small interfering RNA (siRNA) used in this study was described previously (31). Transfection was performed using siLentFect (Bio-Rad), according to the manufacturer's protocol.

Isolation of replication complex. The HCV replication complex was isolated from cells by treatment with 50- μ g/ml digitonin at 27°C for 5 min, following treatment with 0.3- μ g/ml proteinase K at 37°C for 5 min as described previously (31).

Purification of recombinant GST-fused CyPB protein. Glutathione S-transferase (GST) and GST-fused CyPB (GST-CyPB) protein expression was induced

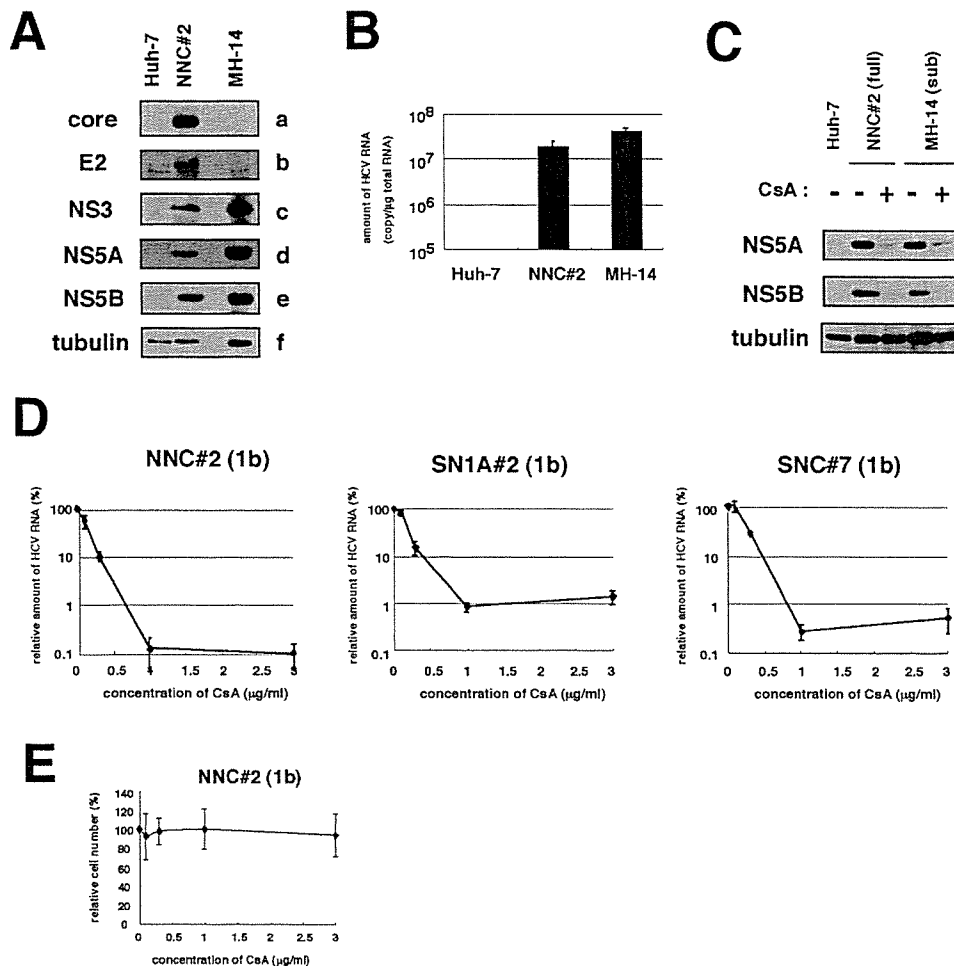


FIG. 2. CsA suppressed the replication of HCV genome, irrespective of the presence of the structural proteins. (A) Detection of HCV proteins from NNC#2 (NN/1b/FL) genome-length replicon. Core (a), E2 (b), NS3 (c), NS5A (d), NS5B (e), and tubulin (f) in Huh-7, NNC#2 (NN/1b/FL), and MH-14 (NN/1b/SG) cells analyzed by immunoblot analysis are shown. (B) HCV RNA in Huh-7, NNC#2 (NN/1b/FL), and MH-14 (NN/1b/SG) cells quantified by real-time RT-PCR analysis. The data represent the means of three independent experiments. (C) CsA decreased the production of HCV proteins in NNC#2 (NN/1b/FL), as well as in MH-14 (NN/1b/SG) cells. After treatment with 1- μ g/ml CsA (+) for 5 days or without treatment (-), total-cell lysates of NNC#2 (NN/1b/FL) and MH-14 (NN/1b/SG) cells, together with Huh-7 cells as a negative control, were recovered to examine the production of HCV NS5A (top), NS5B (middle), and tubulin as an internal control (bottom) by immunoblot analysis. The same result was obtained at day 7 after treatment. (D) The sensitivity to CsA of HCV genome-length replicon was almost the same as that of the subgenomic replicon. HCV RNA was quantified by real-time RT-PCR analysis using total RNA from NNC#2 (NN/1b/FL), SN1A#2 (Con1/1b/FL), and SNC#7 (Con1/1b/FL) cells treated with various concentrations of CsA for 7 days. The relative amount of HCV RNA was plotted against the concentration of CsA (in micrograms per milliliter). (E) Effect of CsA on cell proliferation. NNC#2 (NN/1b/FL) cells were treated with various amount of CsA for 7 days. Cell numbers were counted, and cell numbers relative to those of cells without treatment were plotted against the concentration of CsA.

in transformed BL21 cells (Amersham) with 1 mM isopropyl- β -thiogalactopyranoside (IPTG). The cell lysate was incubated with glutathione-Sepharose resin (Amersham) and washed extensively. The recombinant protein was eluted by glutathione (pH 8.0) and subsequently dialyzed.

In vitro RNA binding assay. In vitro-translated ³⁵S-labeled NS5B proteins and poly(U)-Sepharose (Amersham) or protein G-Sepharose (Amersham) resin as a negative control were incubated in the presence of recombinant GST-CyPB protein at 4°C for 1 h. After being washed, precipitates were fractionated by sodium dodecyl sulfate-polyacrylamide gel electrophoresis and analyzed by imaging analyzer.

RESULTS

CsA suppressed the replication of HCV full-genome replicon. We and another group have reported an anti-HCV activ-

ity of CsA using subgenomic replicons (22, 29). HCV structural proteins, especially the core protein, have multiple functions. These proteins interact with many cellular factors and modulate a variety of cellular functions (32). Potentially, these viral proteins could diminish or circumvent the suppression of HCV genome replication by CsA. Core protein and E2 reportedly modulate the activity of IFN signaling (9, 25). To test this possibility, we established a full-genome HCV replicon system with cells transfected with the NN strain (NNC#2 cells [NN/1b/FL]) (Fig. 1). HCV RNA and protein productions were confirmed by real-time RT-PCR and immunoblot analysis (Fig. 2A and B). In addition, we confirmed that this replication was not due to the integration of the replicon construct into the

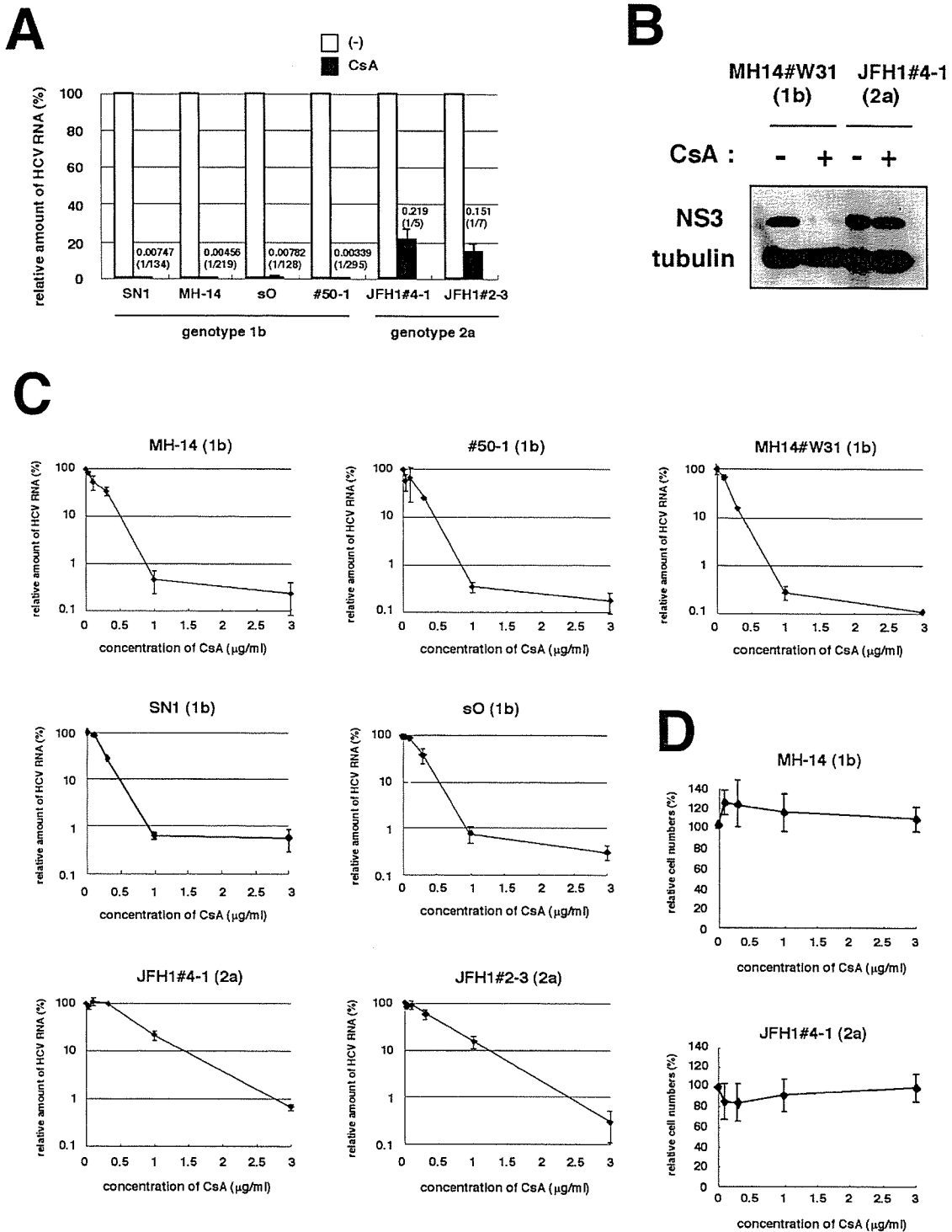


FIG. 3. Replication of a genotype 2a strain, JFH1, was less sensitive to CsA. (A) Sensitivity to CsA of HCV genotype 1b and JFH1 replicons. SN1 (Con1/1b/SG), MH-14 (NN/1b/SG), sO (O/1b/SG), #50-1 (NN/1b/SG), JFH1#4-1 (JFH1/2a/SG), and JFH1#2-3 (JFH1/2a/SG) cells, carrying HCV subgenomic replicon, were treated with 1- μ g/ml CsA for 7 days. HCV RNA titers were quantified by real-time RT-PCR analysis, and the relative amounts are shown. The bars represent the means of three independent experiments. White bars, no treatment; black bars, 1- μ g/ml CsA. The numbers above the black bars indicate fold difference of the titer with 1- μ g/ml CsA treatment compared to no treatment. (B) Levels of NS3 and tubulin as an internal control in MH14#W31 (NN/1b/SG) and JFH1#4-1 (JFH1/2a/SG) cells without (-) or with (+) 1- μ g/ml CsA treatment for 5 days were detected by immunoblot analysis. (C) HCV RNA was quantified and plotted as described in the legend to Fig. 2D with genotype 1b replicon cells such as MH-14 (NN/1b/SG), #50-1 (NN/1b/SG), MH14#W31 (NN/1b/SG), SN1 (Con1/1b/SG), and sO (O/1b/SG) cells and JFH1-carrying replicon cells such as JFH1#4-1 (JFH1/2a/SG) and JFH1#2-3 (JFH1/2a/SG) cells. (D) Effect of CsA on cell proliferation. The growth of MH-14 (NN/1b/SG) and JFH1#4-1 (JFH1/2a/SG) cells were examined as described in the legend for Fig. 2E.

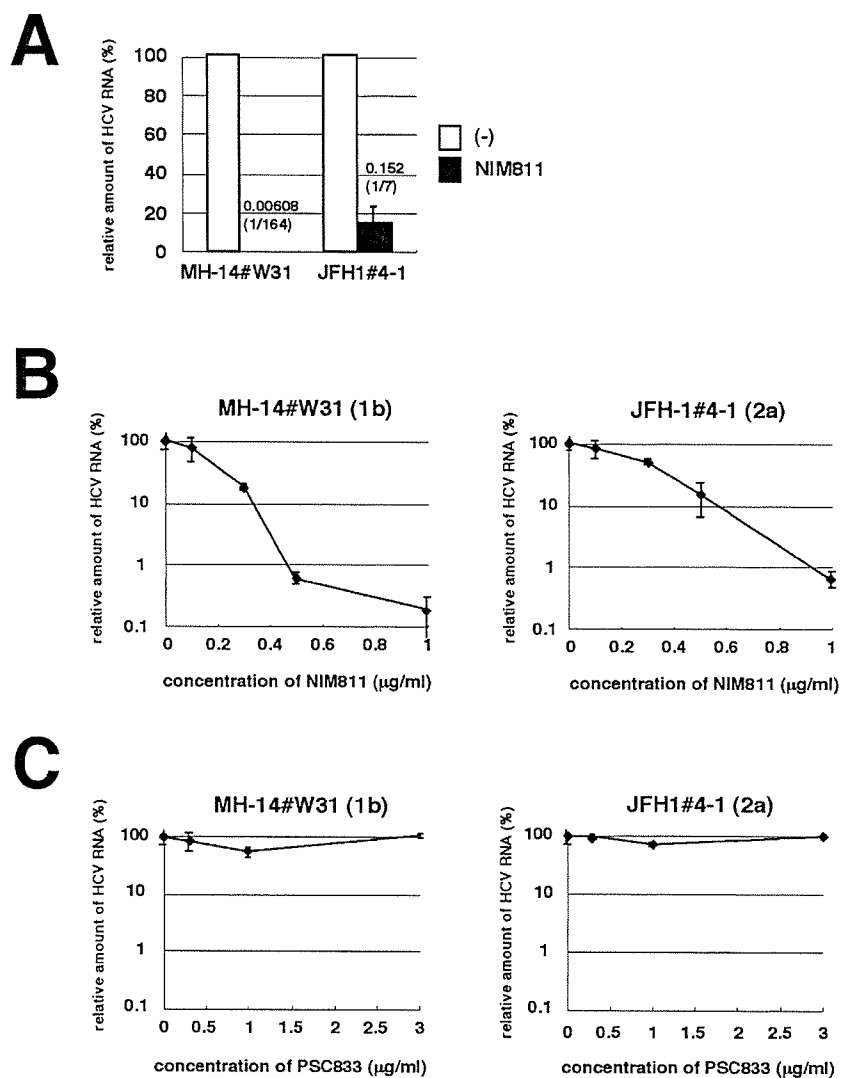


FIG. 4. JFH1 replication was less sensitive to a CsA derivative, NIM811. (A) MH14#W31 (NN/1b/SG) and JFH1#4-1 (JFH1/2a/SG) cells were treated with 0.5- $\mu\text{g/ml}$ NIM811 for 7 days. HCV RNA titers were quantified as described in the legend to Fig. 3A. White bars, no treatment; black bars, 0.5- $\mu\text{g/ml}$ NIM811. (B and C) HCV RNA in replicon cells treated with various concentrations of NIM811 (B) or PSC833 (C) for 7 days was quantified and plotted against the concentration of NIM811 (B) or PSC833 (C) (in micrograms per milliliter) as described in the legend to Fig. 3C.

cellular genome (data not shown). Similarly, we generated other full-genome replicon cells carrying sequences from the Con1 strain at the nonstructural coding region of the replicon RNA (SN1A#2 [Con1/1b/FL]) and SNC#7 (Con1/1b/FL) cells (Fig. 1). The replicon of SN1A#2 (Con1/1b/FL) cells possessed the EMCV IRES upstream of the open reading frame for HCV proteins, while that of SNC#7 (Con1/1b/FL) cells contained the HCV IRES (Fig. 1). SNC#7 (Con1/1b/FL) cells exhibited almost the same response as that of SN1A#2 (Con1/1b/FL) cells to CsA treatment (Fig. 2D). Consistent with a previous report (22), the EMCV IRES was not responsible for the anti-HCV activity of CsA. We compared the sensitivity to CsA of full-genome replicons with that of subgenomic replicons. CsA strongly decreased the production of HCV proteins in both the full-genome replicon, NNC#2 (NN/1b/FL) cells and the subgenomic replicon, MH-14 (NN/1b/SG)

cells (Fig. 2C). Real-time RT-PCR analysis also revealed a dramatic reduction of the RNA level of full-genome replicons in NNC#2 (NN/1b/FL), SN1A#2 (Con1/1b/FL), and SNC#7 (Con1/1b/FL) cells (Fig. 2D). The 50% inhibitory concentrations (IC_{50}) of CsA in NNC#2 (NN/1b/FL), SN1A#2 (Con1/1b/FL), and SNC#7 (Con1/1b/FL) cells were estimated to be 0.13, 0.19, and 0.24 $\mu\text{g/ml}$, respectively. The 90% inhibitory concentrations (IC_{90}) of CsA in these cells were 0.68, 0.94, and 0.81 $\mu\text{g/ml}$, respectively. The CsA dose-response curves of full-genome replicons and subgenomic replicons were similar (i.e., compare SN1A#2 or SNC#7 [Con1/1b/FL] versus SN1 [Con1/1b/SG], NNC#2 [NN/1b/FL] versus MH-14, #50-1, or MH14#W31 [NN/1b/SG]) (Fig. 3C). These results demonstrate that CsA suppresses the replication of full-genome replicons and subgenomic replicons to almost the same extent. Since CsA concentrations of up to 3 $\mu\text{g/ml}$ did not affect the

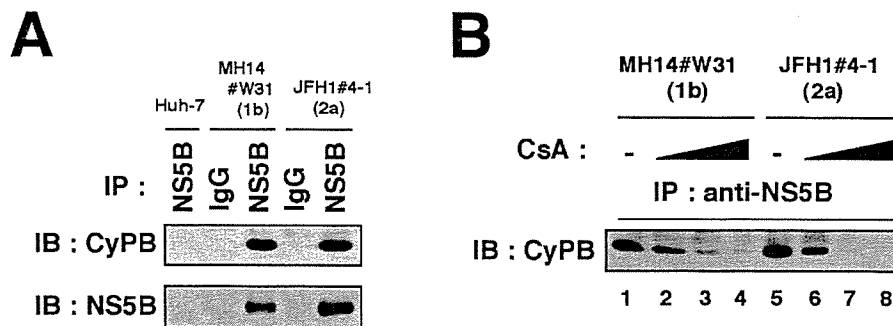


FIG. 5. Interaction of HCV NS5B with CyPB in the JFH1 replicon. (A) Coimmunoprecipitation of endogenous CyPB with NS5B. Lysates from MH14#W31 (NN/1b/SG), JFH1#4-1 (JFH1/2a/SG), and Huh-7 cells as a negative control were used for immunoprecipitation with normal mouse immunoglobulin G (IgG) or anti-NS5B antibody (NS5B), followed by immunoblot analysis with either anti-CyPB (top) or anti-NS5B antibodies (bottom). IP, antibodies used for immunoprecipitation. (B) The interaction of CyPB with NS5B in JFH1 replicon was disrupted by CsA treatment. Coimmunoprecipitation between CyPB and NS5B was analyzed with MH14#W31 (NN/1b/SG) or JFH1#4-1 (JFH1/2a/SG) cells treated without CsA (lanes 1 and 5) or with CsA (0.3 $\mu\text{g}/\text{ml}$ in lanes 2 and 6, 1 $\mu\text{g}/\text{ml}$ in lanes 3 and 7, and 3 $\mu\text{g}/\text{ml}$ in lanes 4 and 8).

proliferation of any replicon cells (Fig. 2E and data not shown), the effect of CsA on replication is not due to the cytotoxic effect. In addition, we observed the reduction of production of infectious viral particles in the presence of 3- $\mu\text{g}/\text{ml}$ CsA (data not shown) using the viral production system with full-genome JFH1 RNA (27).

The JFH1 replicon was less sensitive to CsA than were genotype 1b replicons. We compared the sensitivity of HCV replication to CsA in several subgenomic replicon cells. We used MH-14 (NN/1b/SG) and #50-1 (NN/1b/SG) cells carrying subgenomic replicons with HCV NN strain (15, 29), SN1 (Con1/1b/SG) cells carrying the Con1 subgenomic replicon (18), and sO (O/1b/SG) cells bearing the subgenomic O strain (12) as genotype 1b replicon-containing cells. We also employed JFH1#4-1 (JFH1/2a/SG) and JFH1#2-3 (JFH1/2a/SG) cell clones carrying the JFH1 subgenomic replicon (13). Treatment of CsA (1 $\mu\text{g}/\text{ml}$; 7 days) drastically decreased HCV RNA in all the subgenomic replicon cells carrying the HCV genotype 1b strain. HCV RNA levels in SN1 (Con1/1b/SG), MH-14 (NN/1b/SG), sO (O/1b/SG), and #50-1 (NN/1b/SG) cells decreased to 1/134, 1/219, 1/128, and 1/295, respectively (Fig. 3A). Genotype 1b replicon cells appeared highly sensitive to CsA. In contrast, the effect of CsA on HCV RNA levels in replicon cells containing sequences from the JFH1 strain was limited to 1/5 to 1/7 (Fig. 3A). These results of the response to CsA were reproduced in further additional cell clones.

The cellular characteristics of Huh-7 cell strains differ among laboratories. To exclude the possibility that differences between Huh-7 cell strains influence the sensitivity to CsA, we established genotype 1b replicon cells based on the identical Huh-7 cell strain, which were used as parental cells of JFH1#4-1 (JFH1/2a/SG) and JFH1#2-3 (JFH1/2a/SG) cells. The response of the corresponding replicon cells, MH14#W31 (NN/1b/SG), to CsA was almost the same as that of SN1 (Con1/1b/SG), MH-14 (NN/1b/SG), sO (O/1b/SG), and #50-1 (NN/1b/SG) cells (Fig. 3C). Thus, the difference in sensitivity of JFH1 and genotype 1b strains to CsA can be attributed to the characteristic differences of the HCV strains, not to the parental Huh-7 cell strain. In addition, the reduction of NS3 protein in JFH1#4-1 (JFH1/2a/SG) cells following treatment

with CsA was less prominent than that in MH14#W31 (NN/1b/SG) cells (Fig. 3B).

We examined the dose-response curve of HCV RNA against the concentration of CsA (Fig. 3C). The effect of CsA in genotype 1b replicons plateaued at around 1 $\mu\text{g}/\text{ml}$, while in the dose-response curve in JFH1 replicon, the inhibition was not yet saturated (Fig. 3C). As concentrations of CsA up to 3 $\mu\text{g}/\text{ml}$ did not affect the proliferation rate of any replicon cells (Fig. 3D and data not shown), the effect of CsA on replication was not due to the cytotoxic effect. The IC_{50} of CsA in MH-14 (NN/1b/SG), #50-1 (NN/1b/SG), MH14#W31 (NN/1b/SG), SN1 (Con1/1b/SG), sO (O/1b/SG), JFH1#4-1 (JFH1/2a/SG), and JFH1#2-3 (JFH1/2a/SG) cells were estimated to be 0.15, 0.18, 0.16, 0.20, 0.25, 0.67, and 0.43 $\mu\text{g}/\text{ml}$, respectively. The IC_{90} was 0.86, 0.82, 0.76, 0.88, 0.92, 2.77, and 2.39 $\mu\text{g}/\text{ml}$, respectively. A similar dose-response curve in the JFH1 replicon was obtained by a transient replication assay with the luciferase reporter driven from a JFH1 replicon construct (data not shown) (14).

JFH1 replicon was less sensitive to a CsA derivative, NIM811. Analysis of several CsA derivatives has revealed that the anti-HCV effect of CsA on the genotype 1b replicon is mediated by the inhibition of CyP (31). We examined the sensitivity of JFH1 replicon to CsA derivatives. CsA is known to have three major cellular targets: CyP, calcineurin (CN)/NF-AT, and P glycoprotein (P-gp) (28, 31). A CsA derivative, NIM811, inhibits CyP and P-gp but not CN/NF-AT, while another derivative, PSC833, inhibits P-gp but neither CyP nor CN/NF-AT (31). The decrease of HCV RNA in MH14#W31 (NN/1b/SG) cells with NIM811 treatment (0.5 $\mu\text{g}/\text{ml}$; 7 days) was more than an order of magnitude greater than that in JFH1#4-1 (JFH1/2a/SG) cells (Fig. 4A). The slope of the dose-response curve of NIM811 treatment of the JFH1 replicon was gentler than that of genotype 1b (Fig. 4B). The IC_{50} of NIM811 in MH14W#31 (NN/1b/SG) and JFH1#4-1 (JFH1/2a/SG) cells were 0.17 and 0.30 $\mu\text{g}/\text{ml}$, respectively. The IC_{90} were 0.46 and 0.93 $\mu\text{g}/\text{ml}$, respectively. In contrast, PSC833, which does not inhibit CyP, did not alter HCV RNA level in either genotype 1b or the JFH1 replicon (Fig. 4C). Thus, a CyP

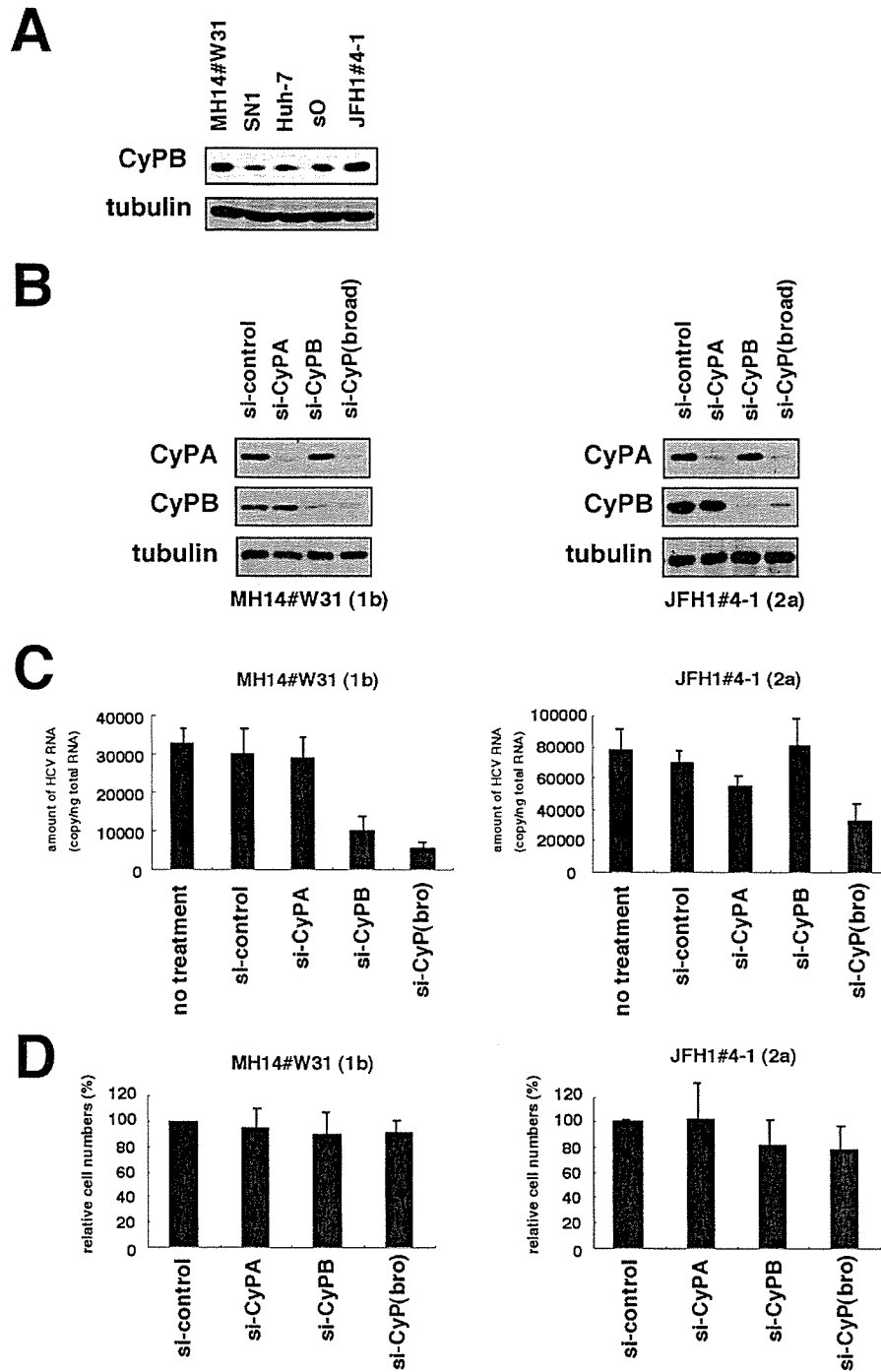


FIG. 6. CyPB in HCV replication of genotype 1b and JFH1. (A) Expression level of endogenous CyPB protein (top) and tubulin as an internal control (bottom) in MH14#W31 (NN/1b/SG), SN1 (Con1/1b/SG), sO (O/1b/SG), JFH1#4-1 (JFH1/2a/SG), and Huh-7 cells. (B) Knockdown of endogenous CyP proteins. MH14#W31 (NN/1b/SG) and JFH1#4-1 (JFH1/2a/SG) cells were transfected with siRNA specific for CyPA (si-CyPA), CyPB (si-CyP), a broad range of CyP subtypes [si-CyP(broad)], or a randomized siRNA (si-control). At 72 h posttransfection, CyPA (top), CyPB (middle) and tubulin as an internal control (bottom) were detected in total cell lysates of MH14#W31 (NN/1b/SG) (left) and JFH1#4-1 (JFH1/2a/SG) (right) cells by immunoblot analysis. (C) Depletion of CyPB did not affect HCV replication of JFH1 replicon. At 5 days posttransfection, HCV RNA titers in MH14#W31 (NN/1b/SG) (left) and JFH1#4-1 (JFH1/2a/SG) (right) cells were quantified by real-time RT-PCR analysis. no treatment, treatment with only the transfection reagent in the absence of siRNA. (D) Effect of siRNA on cell proliferation. Cell numbers of MH14W#31 (NN/1b/SG) and JFH1#4-1 (JFH1/2a/SG) cells treated with siRNA for 5 days were counted. Relative cell numbers were indicated.

inhibitor was less effective at suppressing the replication of the JFH1 replicon than genotype 1b replicons.

Interactions between CyPB and JFH1 NS5B. Previously, we have shown that CyPB interacts with NS5B to promote HCV genome replication and that CsA inhibits this binding in a genotype 1b replicon (31). Here, we examined the association between CyPB and NS5B in a JFH1 replicon. Immunoprecipitation analysis revealed an interaction of CyPB with NS5B in JFH1#4-1 (JFH1/2a/SG) cells (Fig. 5A). This interaction was dissociated following the treatment of CsA, as observed with the genotype 1b replicon (Fig. 5B).

Role of CyPB in replication of the JFH1 replicon. Although we observed some differences of expression levels of endogenous CyPB among the replicon cells in the immunoblot analysis (Fig. 6A), there was no particular correlation between endogenous CyPB expression levels and replication sensitivity to CsA among cells. CyPB reportedly regulates HCV genome replication of the genotype 1b replicon (31). We then explored the requirement of CyPB for the replication of JFH1 replicon with RNA interference. Transfecting siRNAs designed to recognize several CyP subtypes [si-CyP(broad)] (Fig. 6B) reduced HCV RNA to $<1/5$ in MH14#W31 (NN/1b/SG) cells (Fig. 6C). Specific knockdown of CyPB but not CyPA (Fig. 6B) decreased HCV RNA in MH14#W31 (NN/1b/SG) cells, consistent with a previous report (Fig. 6C) (31). In contrast, HCV RNA in JFH1#4-1 (JFH1/2a/SG) cells was not altered following the suppression of either endogenous CyPA or CyPB (Fig. 6B and C). We observed a weak decrease of HCV RNA levels (around one-half) with si-CyP(broad) (Fig. 6C). These data suggests the possibility that the replication of the JFH1 replicon is independent of CyPB, in contrast to the genotype 1b replicon. In the previous study, it was reported that the doubling time, saturation density, and response to cell confluence of the replicon cells carrying JFH1 were different from those in cells carrying a genotype 1b replicon, suggesting the possibility that the coupling relationship between the replication and cell growth was different between genotype 1b and the JFH1 replicon (21). The introduction of either si-CyPB or si-CyP(broad), however, had little effect on cell growth in MH14#W31 (NN/1b/SG) or JFH1#4-1 (JFH1/2a/SG) cells (Fig. 6D). And we did not observe cells being confluent in the experiment period. The above results suggest that the different response to si-CyPB in the two lines is independent of the conditions of cell growth.

The role of CyPB in the RNA binding activity of JFH1 NS5B. CyPB regulates HCV genome replication of a genotype 1b replicon by promoting the RNA binding activity of NS5B (31). We examined the effect of CyPB on the RNA binding activity of NS5B in JFH1. NS5B in the replication complex was isolated from cells by treatment with digitonin-proteinase K, as described previously (31). This fraction was incubated with poly(U) RNA-Sepharose or protein G-Sepharose as a negative control for the detection of RNA binding NS5B in the replication complex. RNA-bound NS5B in this fraction from MH14#W31 (NN/1b/SG) cells was decreased drastically following treatment with CsA (Fig. 7A, lanes 5 and 6). However, the reduction of RNA binding of NS5B in the replication complex of JFH1#4-1 (JFH1/2a/SG) cells was not as prominent (Fig. 7A, lanes 11 and 12). We confirmed this result by an in vitro RNA binding assay, in which in vitro-synthesized NS5B was incubated with poly(U) RNA-Sepharose, together with

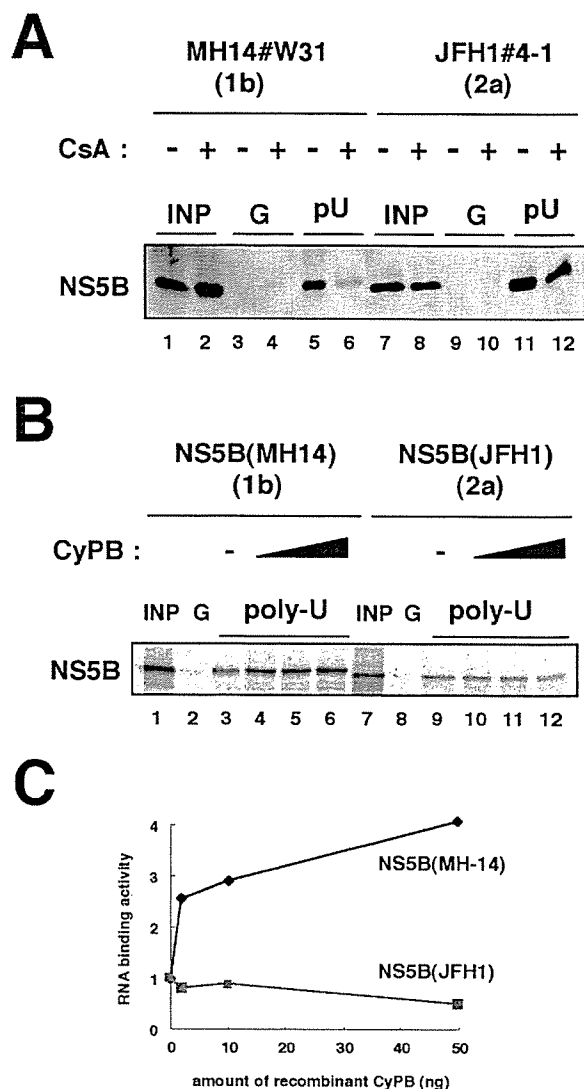


FIG. 7. RNA binding capacity of JFH1 NS5B was independent of CyPB. (A) An RNA-protein binding precipitation assay was performed using MH14#W31 (NN/1b/SG) cells (lanes 1 to 6) and JFH1#4-1 (JFH1/2a/SG) cells (lanes 7 to 12) as described in Materials and Methods. MH14#W31 (NN/1b/SG) and JFH1#4-1 (JFH1/2a/SG) cells preincubated without (lanes 1, 3, 5, 7, 9, and 11) or with (lanes 2, 4, 6, 8, 10, and 12) CsA were treated with digitonin, followed by digestion with proteinase K to isolate the replication complex. This fraction was then incubated with poly(U) RNA-Sepharose (lanes 5, 6, 11, and 12) or protein G-Sepharose as a negative control (lanes 3, 4, 9, and 10). Precipitates were detected by immunoblot analysis with anti-NS5B antibody. INP, one-sixth of the amount of cell lysate used in the precipitation assay; G and pU, samples with protein G-Sepharose and poly(U)-Sepharose, respectively. (B) An in vitro RNA binding assay was performed as described in Materials and Methods. In vitro-synthesized NS5B of MH-14 (lanes 1 to 6) or JFH1 (lanes 7 to 12) with the rabbit reticulocyte lysate in the presence of [35 S]methionine was incubated with protein G-Sepharose (lanes 2 and 8) or poly(U)-Sepharose in the absence (lanes 3 and 9) or presence of various amounts of purified recombinant GST-CyPB (2 ng in panels 4 and 10, 10 ng in panels 5 and 11, and 50 ng in panels 6 and 12). The resultant precipitates were fractionated by sodium dodecyl sulfate-polyacrylamide gel electrophoresis, followed by the detection of radiolabeled protein. (C) The density of the bands of NS5B in the RNA binding fraction was quantified and plotted against the amount of the recombinant GST-CyPB (in nanograms). Solid line, NS5B of MH-14; faint line, NS5B of JFH1.

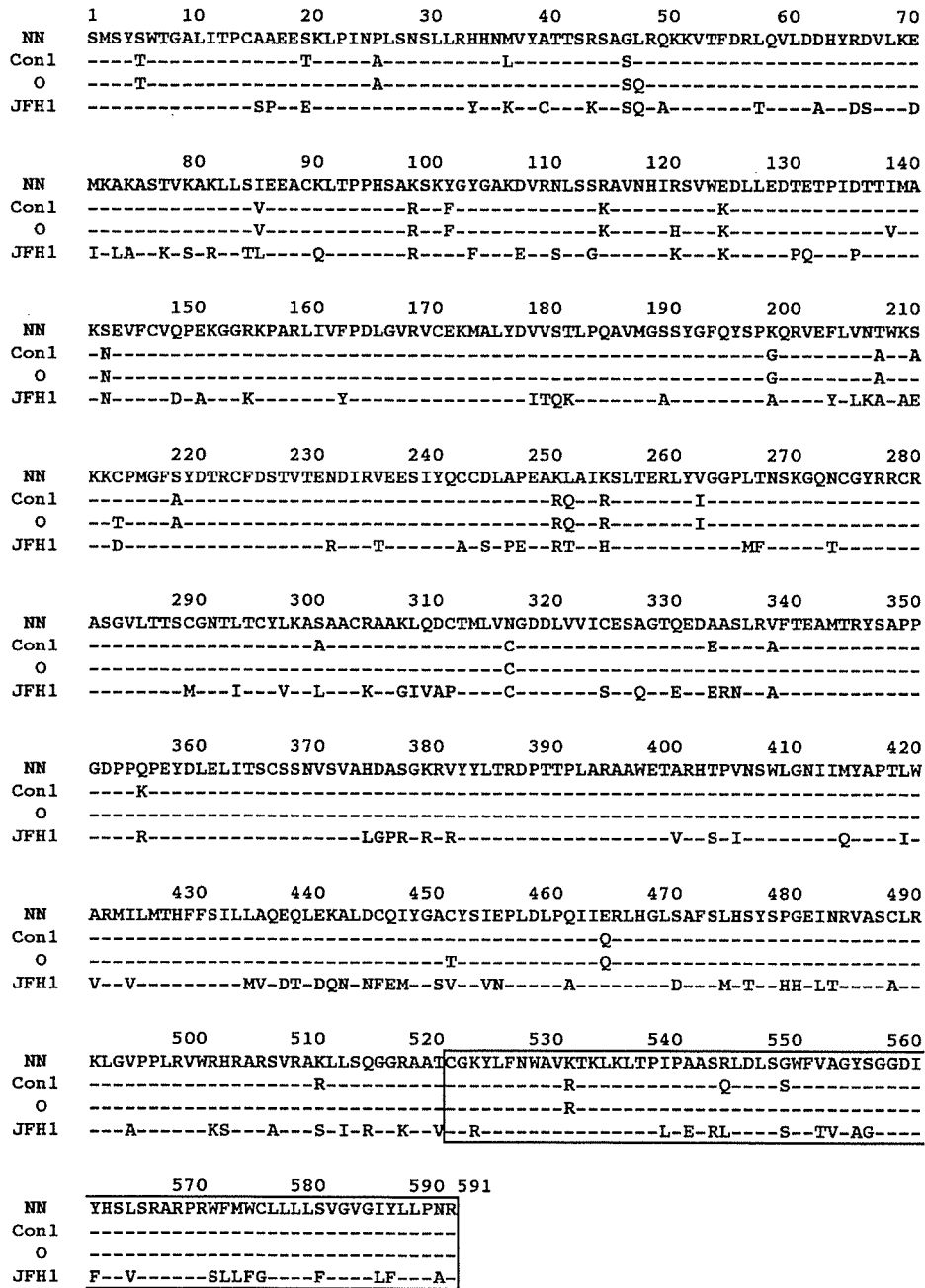


FIG. 8. Amino acid sequence alignment of NS5B encoded by HCV strains NN, Con1, O, and JFH1. The numbers above the sequence indicate the amino acid numbers. Conserved residues are shown by dashes. The region spanning 521 to 591 aa, which is involved in the interaction with CyPB, is boxed.

recombinant GST-CyPB. The addition of recombinant GST-CyPB increased the binding of genotype 1b NS5B to poly(U) RNA (Fig. 7B and C). However, this augmentation of RNA binding was not observed with NS5B from the JFH1 strain (Fig. 7B and C). From the above results, it is suggested that the RNA binding of JFH1 NS5B is free from regulation by CyPB.

DISCUSSION

Until now, we and another group have utilized subgenomic replicons carrying genotype 1b NN and HCV-N strains to

demonstrate that CsA suppresses HCV genome replication (22, 29). This study reveals that CsA is effective on full-genome replicons to almost the same extent. In addition, other available genotype 1b replicons carrying the Con1 and O strains also have a high sensitivity to CsA, consistent with our proposal that HCV genotype 1b is highly sensitive to CsA. However, a fulminant-type genotype 2a replicon, JFH1, was less responsive to CsA, although a high dose of CsA suppressed the replication of this strain.

CyPB interacts with genotype 1b NS5B to stimulate its RNA

binding activity. In contrast, CyPB binds JFH1 NS5B but does not regulate the function of JFH1 NS5B. This is consistent with a previous speculation that genotype 1b and JFH1 replicons utilize the same cellular factors in distinct manners (21). The NS5B sequence of NN strain has 95.0, 95.9, and 70.4% homology to that of Con1, O, and JFH1, respectively (Fig. 8). The region spanning amino acids (aa) 521 to 591 of NS5B, which is involved in the interaction with CyPB (31), is highly conserved among genotype 1b strains NN, Con1, and O while that of JFH1 has 21 substituted residues in this region. The proline at 540 aa, which is important for CyPB binding (31), is conserved but the adjacent residues such as isoleucine at 539 aa and alanine at 541 aa are replaced by leucine and glutamic acid, respectively, in JFH1. Through molecular interactions, CyPB seems to make the conformation of NS5B of genotype 1b strains but not JFH1 suitable for RNA binding (31). The diverse regulation system of NS5B by CyPB among strains may be due to differences in either the sequence or the entire conformation of NS5B. Further study is important for elucidating the regulation mechanism of RNA binding activity of NS5B by CyPB.

Thus, replication in JFH1 replicon is independent of CyPB. Interestingly, human immunodeficiency virus type 1 (HIV-1) strains also have a diversity of CyP dependence on viral proliferation (3, 33). CyPA plays an important role in the life cycle of HIV-1. The interaction of the HIV-1 capsid protein with CyPA that resides within the target cells of infection is critical for HIV-1 replication (7, 24). In peripheral blood mononuclear cells or Jurkat T cells, CsA suppresses the proliferation of HIV-1 group main (M) strain (3). However, certain strains of group outlier (O), such as MVP5180 and MVP9435, are resistant to CsA (3, 33), suggesting the different dependency of the replication on CyPA. Authors have suggested that MVP5180 and MVP9435 clones adapt to replicate independently of CyPA and that this adaptation provides a significant replication advantage for the virus in vivo (3). In vesicular stomatitis virus (VSV) strains, a role for CyPA in virus replication also has been reported (2). CyPA is required for the infection of the VSV-NJ strain but not the VSV-IND strain. These authors proposed that during evolutionary divergence from the ancestral lineages that initially were dependent on CyPA for replication, VSV-IND may have adapted to reduce its dependency on CyPA (2). In the case of HCV, a fulminant type genotype 2a replicon (JFH1) replicates independently of CyPB. It has previously been reported that JFH1 has a much higher competency of replication in the cells than other strains (13). The adaptation to independence from CyPB may contribute to the high capacity of replication of JFH1.

Although the JFH1 replicon is less sensitive to CsA, high concentrations of CsA still suppress replication of the JFH1 replicon. Moreover, the introduction of the siRNA designed to recognize several CyP subtypes [si-CyP(broad)] moderately diminishes HCV RNA in the JFH1 replicon. We suspect that a CyP family member other than CyPB is involved in HCV genome replication. Further analysis is needed on the role of other CyP subtypes.

As there a replicon system for a fulminant-type genotype 1b replicon or chronic-type genotype 2a replicon does not yet exist, we cannot conclude whether chronic-type genotype 2a replicons or fulminant-type replicons are less sensitive to CsA

or not. However, there is a clinical report describing cotreatment of patients with chronic hepatitis C with IFN and CsA that resulted in a higher sustained virological rate than with treatment of IFN alone (11). In this report, increase in the sustained virological rate was prominent with patients carrying genotype 1 HCV (51.7% versus 21.9%), while it was relatively weak in patients carrying genotype 2 HCV (66.7% versus 58.3%) (11). Thus, genotype may affect the sensitivity of HCV replication to CsA. However, we cannot exclude the possibility that the diminished sensitivity to CsA is a characteristic only of the fulminant-type genotype 2a strain.

Our results suggest that sensitivity to CsA and replication dependency to CyPB is different among HCV strains. This finding is an important insight into the diversity of the mechanism of HCV genome replication and its sensitivity to antiviral agents.

ACKNOWLEDGMENTS

We thank H. Takahashi and M. Hosaka for preparing replicon cells and generating plasmids. We are grateful to A. Takamizawa at Osaka University, I. Fukuya at Osaka University, and M. Kohara at Tokyo Metropolitan Institute of Medical Science for antibodies and R. Bartenschlager at Heiderberg University for the I377/NS3-3' sequence. We also appreciate Novartis (Basel, Switzerland) for providing the CsA derivatives NIM811 and PSC833.

This work was supported by grants-in-aid for cancer research and for the second-term comprehensive 10-year strategy for cancer control from the Ministry of Health, Labor, and Welfare; grants-in-aid for scientific research from the Ministry of Education, Culture, Sports, Science and Technology; and grants-in-aid from the Research for the Future from the Japanese Society for the Promotion of Science, the Program for Promotion of Fundamental Studies in Health Science of the Organization for Pharmaceutical Safety and Research of Japan, and Research on Health Sciences focusing on Drug Innovation from the Japan Health Sciences Foundation.

REFERENCES

- Bartenschlager, R., and V. Lohmann. 2001. Novel cell culture systems for the hepatitis C virus. *Antiviral Res.* 52:1-17.
- Bose, S., M. Mathur, P. Bates, N. Joshi, and A. K. Banerjee. 2003. Requirement for cyclophilin A for the replication of vesicular stomatitis virus New Jersey serotype. *J. Gen. Virol.* 84:1687-1699.
- Braaten, D., E. K. Franke, and J. Luban. 1996. Cyclophilin A is required for the replication of group M human immunodeficiency virus type 1 (HIV-1) and simian immunodeficiency virus STV_{CPZ}GAB but not group O HIV-1 or other primate immunodeficiency viruses. *J. Virol.* 70:4220-4227.
- Bukh, J., R. H. Purcell, and R. H. Miller. 1994. Sequence analysis of the core gene of 14 hepatitis C virus genotypes. *Proc. Natl. Acad. Sci. USA* 91:8239-8243.
- Frese, M., V. Schwarzle, K. Barth, N. Krieger, V. Lohmann, S. Mihm, O. Haller, and R. Bartenschlager. 2002. Interferon-gamma inhibits replication of subgenomic and genomic hepatitis C virus RNAs. *Hepatology* 35:694-703.
- Grakoui, A., C. Wychowski, C. Lin, S. M. Feinstone, and C. M. Rice. 1993. Expression and identification of hepatitis C virus polyprotein cleavage products. *J. Virol.* 67:1385-1395.
- Hatzioannou, T., D. Perez-Caballero, S. Cowan, and P. D. Bieniasz. 2005. Cyclophilin interactions with incoming human immunodeficiency virus type 1 capsids with opposing effects on infectivity in human cells. *J. Virol.* 79:176-183.
- Hijikata, M., H. Mizushima, T. Akagi, S. Mori, N. Kakiuchi, N. Kato, T. Tanaka, K. Kimura, and K. Shimotohno. 1993. Two distinct proteinase activities required for the processing of a putative nonstructural precursor protein of hepatitis C virus. *J. Virol.* 67:4665-4675.
- Hosui, A., K. Ohkawa, H. Ishida, A. Sato, F. Nakanishi, K. Ueda, T. Takehara, A. Kasahara, Y. Sasaki, M. Hori, and N. Hayashi. 2003. Hepatitis C virus core protein differently regulates the JAK-STAT signaling pathway under interleukin-6 and interferon-gamma stimuli. *J. Biol. Chem.* 278:28562-28571.
- Ikeda, M., M. Yi, K. Li, and S. M. Lemon. 2002. Selectable subgenomic and genome-length dicistronic RNAs derived from an infectious molecular clone of the HCV-N strain of hepatitis C virus replicate efficiently in cultured Huh7 cells. *J. Virol.* 76:2997-3006.
- Inoue, K., K. Sekiyama, M. Yamada, T. Watanabe, H. Yasuda, and M.